INSTITUTO SUPERIOR DE ENGENHARIA DO PORTO
MESTRADO EM ENGENHARIA QUÍMICA




Beta-glucanos e manoproteínas do excedente de levedura cervejeira para formulação de filmes biodegradáveis e edíveis aplicados à indústria alimentar

LUÍS ANDRÉ MOREIRA MENDES
Outubro de 2020

POLITÉCNICO
DO PORTO

INSTITUTO SUPERIOR DE ENGENHARIA DO PORTO
MESTRADO EM ENGENHARIA QUÍMICA

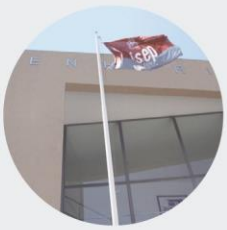


β-glucanos e manoproteínas do excedente de levedura cervejeira para formulação de filmes biodegradáveis e edíveis aplicados à indústria alimentar

LUÍS ANDRE MOREIRA MENDES

outubro de 2020

POLITÉCNICO
DO PORTO

β-glucans and mannoproteins from brewer´s spent yeast in the development of edible films/ coatings for food applications

β-glucanos e manoproteínas do excedente de levedura cervejeira para formulação de filmes biodegradáveis e edíveis aplicados à indústria alimentar

Luís André Moreira Mendes

Dissertação submetida para a obtenção do grau de Mestre em Engenharia Química, ramo opcional Energia e Biorrefinaria

Orientadoras:
Professora Doutora Cristina Delerue-Matos
Doutora Elsa F. Vieira

Centro de investigação: GRAQ – Grupo de Reação e Análises Químicas

Outubro de 2020

Agradecimentos

Após a realização desta dissertação de Mestrado, não poderia deixar de agradecer a todos os que me ajudaram e acompanharam durante estes últimos meses.

Agradeço ao GRAQ e a todos os seus colaboradores. Gostaria de agradecer, em especial, à Professora Doutora Cristina Delerue-Matos pela simpatia e disponibilidade demonstrada e por ter consentido a minha entrada no grupo de investigação. À Doutora Elsa Vieira por me receber e me integrar de imediato com os investigadores do GRAQ, pela excelente orientação e pelos conselhos dados ao longo da dissertação, bem como a incansável paciência durante os meus momentos mais "teimosos" na escrita da dissertação. Agradeço também ao meu colega, Leonardo Amaral, pelo companheirismo e agilidade em ajudar-me em várias situações de laboratório, quer a procurar material, quer na ajuda em atividades experimentais realizadas, bem como as valiosas sugestões nas atividades práticas que realizei durante o curto espaço de tempo passado em laboratório.

Gostaria também de agradecer à direção do Mestrado em Engenharia Química, composta pela Professora Anabela Guedes e pelos Professores Gilberto Pinto e Hendrikus Nouws, pelo trabalho realizado na organização das dissertações de Mestrado e do ciclo de estudos do curso e pela valiosa partilha de informação de relevo para o meu percurso académico.

Um agradecimento especial à Post Scriptum Brewery, em especial ao mestre cervejeiro Pedro Sousa, pelo fornecimento da levedura e pela atenção demonstrada na visita à sua empresa.

Não poderia deixar de agradecer também aos meus amigos mais próximos que me acompanharam ao longo do meu percurso académico, Amaro Cruz, Cristiano Silva, Daniela Borges, Eduardo Pinho, Miguel Sottomayor e Tiago Fernandes, pela camaradagem e amizade que sempre me proporcionaram, bem como ajuda naquilo que eu mais precisava.

Contudo, o meu maior agradecimento vai para a minha família, que sempre me ajudou e encorajou desde pequeno a seguir os meus sonhos e ambições e que tudo era possível; estou aqui hoje devido à educação exemplar que me deram.

Resumo

A Estratégia Europeia para os Plásticos na Economia Circular refere que até 2030, todas as embalagens plásticas devem ser reutilizáveis ou recicláveis de uma forma economicamente eficiente. Assim, revela-se imperativo o desenvolvimento de soluções de embalagens inteligentes. O presente trabalho apresenta uma revisão bibliográfica sobre a aplicação dos *β*-glucanos e das manoproteínas, oriundos do excedente de levedura cervejeira (*Saccharomyces cerevisiae*), na formulação de filmes edíveis/coatings para aplicação na indústria alimentar. O potencial de mercado para a aplicação de filmes edíveis biodegradáveis e renováveis em embalagens alimentares é enorme e implica o estudo exaustivo das suas propriedades mecânicas, químicas e biológicas. Neste sentido, o capítulo II desta dissertação aborda algumas propriedades dos filmes, com principal destaque para as propriedades antimicrobiana, antioxidante e anti-inflamatória, estabilidade térmica, permeabilidade ao vapor de água e ao oxigénio, e propriedades mecânicas. No capítulo III são abordadas as características estruturais dos *β*-glucanos e das manoproteínas, sendo também explorados os principais métodos de extração e isolamento de *β*-glucanos e das manoproteínas da parede celular da levedura, com enfoque no rendimento extrativo. Reportam-se também as principais propriedades atribuídas aos filmes/coatings preparados a partir de *β*-glucanos e manoproteínas, bem como casos homólogos de filmes compostos por polissacarídeos e proteínas. Por fim, no capítulo IV, é apresentado o atual panorama de aplicação dos *β*-glucanos e manoproteínas na formulação de filmes/coatings para aplicação na indústria alimentar e farmacêutica.

A literatura encontrada refere que os filmes edíveis à base de *β*-glucanos e manoproteínas apresentam propriedades promissoras. Contudo, até ao momento não existe investigação focada no desenvolvimento de um filme edível que combine ambos os compostos. Em teoria, a formulação de um filme à base de *β*-glucanos e manoproteínas não só será compatível com vários plastificantes, como também apresentará um conjunto de propriedades funcionais superiores comparativamente a filmes edíveis convencionais. É sugerido que o uso de diferentes plastificantes pode influenciar os resultados das propriedades do filme edível. Assim, poder-se-á optar por outro plastificante que não seja o convencional (glicerol), como por exemplo polietileno de baixo peso molecular, de forma a obter melhores propriedades mecânicas.

Palavras-Chave: Filme edível/*coating*, *β*-glucanos, manoproteínas, excedente de levedura cervejeira

Summary

The European Strategy for Plastics in a Circular Economy refers that until 2030, all plastic packaging must be reusable or recyclable in an economically efficient way. Therefore, it is of utmost importance to develop smart packaging solutions. The main scope of this dissertation consisted in the investigation of edible films/coatings composed by β-glucans and mannoproteins from brewer's spent yeast (*Saccharomyces cerevisiae*). The market potential for the application of edible films that are biodegradable and renewable in food packaging and encapsulating agents for the pharmaceutical industry appears to be huge. Thus, it is compulsory to study the mechanical, physical, and biological properties of the film. For this effect, at Chapter II, the main film properties were broadly studied, such as antimicrobial and antioxidant activity, thermal stability, water vapor/oxygen permeability, mechanical properties, and anti-inflammatory activity. Chapter III aimed to understand the structural characteristics of β-glucans and mannoproteins, as well as their individual properties. The main extraction and isolation methods of cell wall's β-glucans and mannoproteins are analyzed, as well as their corresponding extractive yield. The main properties obtained in β-glucans and mannoproteins films are also reported, as well as homologous cases of films containing polysaccharides and proteins. Lastly, at Chapter IV, the current industrial landscape in the application of β-glucans and mannoproteins is reviewed, as well as the mention of some industries that commercialize β-glucans and mannoproteins. The patents associated to these two materials are also investigated.

The literature found mentions formulations of edible films of β-glucans and mannoproteins with promising functional properties, revealing in some cases an increase of the food product's shelf-life. However, up to this point there is no investigation focused in developing an edible film that combines the properties of both β-glucans and mannoproteins. Theoretically, the film formulation would present a superior set of functional properties compared to those presented by conventional edible films. It is suggested that using different plasticizers will influence the final properties of edible films. Therefore, in order to obtain more desirable properties, a substitution of the conventional plasticizer (glycerol) can be made, using for example polyethylene glycol of low molecular weight.

Keywords: Edible film/coating, β-glucans, mannoproteins, brewer's spent yeast.

Index

Figure index

Table index

Abbreviations

AFM – Atomic force microscopy

APS – Amylopectin-based starch

COP – Carbon dioxide permeability

DEAE-C – Diethylaminoethyl cellulose

DMA – Dynamic mechanical analysis

DSC – Differential scanning calorimetry

DTA – Differential thermal analysis

EDTA – Ethylenediaminetetraacetic acid

HPMC – Hydroxypropylmethylcellulose

LPS – Lipopolysaccharides

M/G – Mannose/Galactose ratio

MC – Methylcellulose

OP – Oxygen permeability

OPA – Oxygen permeation analyzer

OPC – Oxygen permeability coefficient

OTR – Oxygen transmission rate

PBMC – Peripheral blood mononuclear cells

PEF – Pulsed Electric Field

RH – Relative humidity

RS – Regular starch

S. cerevisiae – *Saccharomyces cerevisiae*

SDS – Sodium dodecyl sulfate

SEM – Scanning electron microscopy

TGA – Thermogravimetric analysis

TMA – Thermomechanical analysis

Tris-HCl – tris(hydroxymethyl)aminomethane hydrochloride

WP – Whey protein

WPI – Isolated whey protein

WVP – Water vapor permeability

WVTR – Water vapor transmission rate

XRD – X-ray diffraction

1 Introduction

At the beginning of the industrial era, the existent polymers were based in renewable resources such as cellulose, cellulose derivates and rubber. Since then, the technological advance of petrochemistry allowed the production of several polymeric materials with similar characteristics to the previous polymers produced. Although it became easy to modify the process and the physical-chemical properties of the polymers, the main limitation of its use is the extreme difficulty in recycle or decompose these materials. To overcome this barrier and replace the non-degradable polymers, several degradable biopolymers were developed. The increased prices of petrochemical materials and the expected reduction in the availability of these materials led to a progressive change in the mindset of major industries. Thus, research was focused on finding polymeric solutions that please all human necessities, considering that the most important factor is the permanent availability of the raw materials required to polymer`s production (Endres & Siebert-Raths, 2011).

In the late 80's and early 90's, several innovative biopolymers were introduced in the market. Despite the encouraging results, these "first generation biopolymers" (*e.g.* polyhydroxyalkanoates obtained from fermentation) were not successfully established in the market, particularly due to incomplete test of some properties, weak economic planning and lack of policies from the largest industrial players to approve its use. After several regulation modifications, new polymers appeared, known as "second generation biopolymers", being like the mass-produced conventional plastics in terms of manufacturing types, properties, and applications (*e.g.* packaging). The most common examples are regenerated cellulose and cellulose derivates, polycaprolactone (PCL) and polyvinylic alcohol (PVA). These polymers were mainly developed for the agricultural and packaging industries. Nowadays, there are many polymeric materials based on the second-generation ones, known as "third generation polymers", presenting a broader field of applications, for example, in the automobile and textile industries. These polymers do not consider the degradability factor so important as it previously was, since the most important factor is now durability. At the same time, there is a progressive support in using renewable resources rather than resources of petrochemical origin. The successive technological advancements in developing these new materials allowed to manipulate properties or variables that were previously impossible to adjust, such as electrical and thermal resistivities, odor, UV stability, among others. A short resume of the characteristics and applications of the first, second and third generation polymers is shown in

Figure 1.

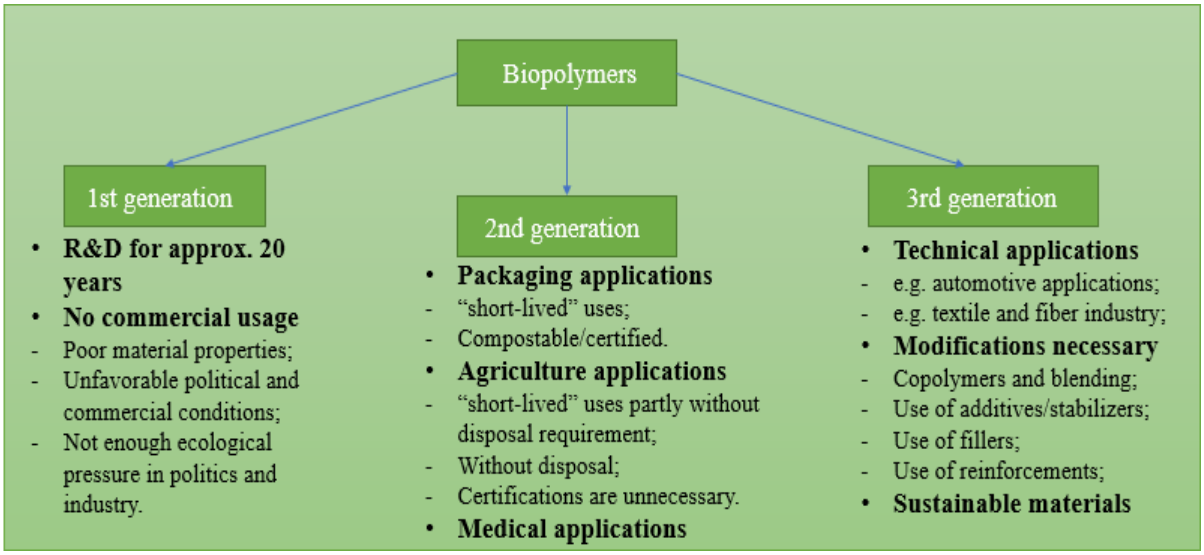

Figure 1 Biopolymer generations and their respective applications **[Adapted from Endres & Siebert-Raths, 2011]**.

The development and management of biodegradable polymers is one of the main emerging trends worldwide. Major companies are adopting biobased and green materials. Similarly, reducing agricultural residues and boosting a circular economy is being endorsed in most countries. The current worldwide packaging market value is around €533 billion. Even substituting 1% of the materials with biodegradable packaging would mean €5 billion. Therefore, there is a tremendous market for biodegradable packaging materials (IPI Singapore). In Europe, the largest application of polymers is destined for packaging, which accounts for almost 40% of the 49 Mt of plastics demand in 2015. EU has been focusing on developing policies to specifically address some of the problematic issues related to plastics. This is the case for the European Strategy for Plastics in a Circular Economy (Watkins & Schweitzer, 2018). Among other objectives, this strategy aims to that all plastics packaging in the EU must be reusable or recyclable in a cost-effective manner by 2030. With this commitment, economy will benefit from being more productive and efficient with all plastic resources and there is a significant potential for Europe to benefit from competitive advantage and job creation opportunities by being at the vanguard of developing more sustainable solutions for plastics (Watkins & Schweitzer, 2018).

In the food packaging sector, the development of edible film/coating based on biopolymers involves the research of their physical-chemical structure. It is important to note

that the concepts "biofilm", "edible film" and "coating" are different; Figure 2 shows an example of each formulation. Biofilm is a microbial three-dimensional structure of multicellular communities (prokaryotic and/or eukaryotic cells) inserted in a matrix made of a microbial-made synthesized material. The biofilm formation is a multiple-stage process that begins from the microbial adhesion with subsequent production and accumulation of an extracellular matrix made of one or more polymeric substrates, like proteins, polysaccharides, extracellular genetic material and humic substance (Azeredo *et al.*, 2017). The concept of coating and edible film seems quite similar; however, the main difference is based on the physical form of its application. An edible coating is applied to the food product in a liquid form, generally by immersion of the food in a solution composed of typical substances of a polymeric matrix (carbohydrates, proteins, lipids, or even a mix of these three substrates). In contrast, the edible film is previously molded in solid and thin "sheets" that are applied as a wrapping in the food product (Falguera *et al.*, 2017).

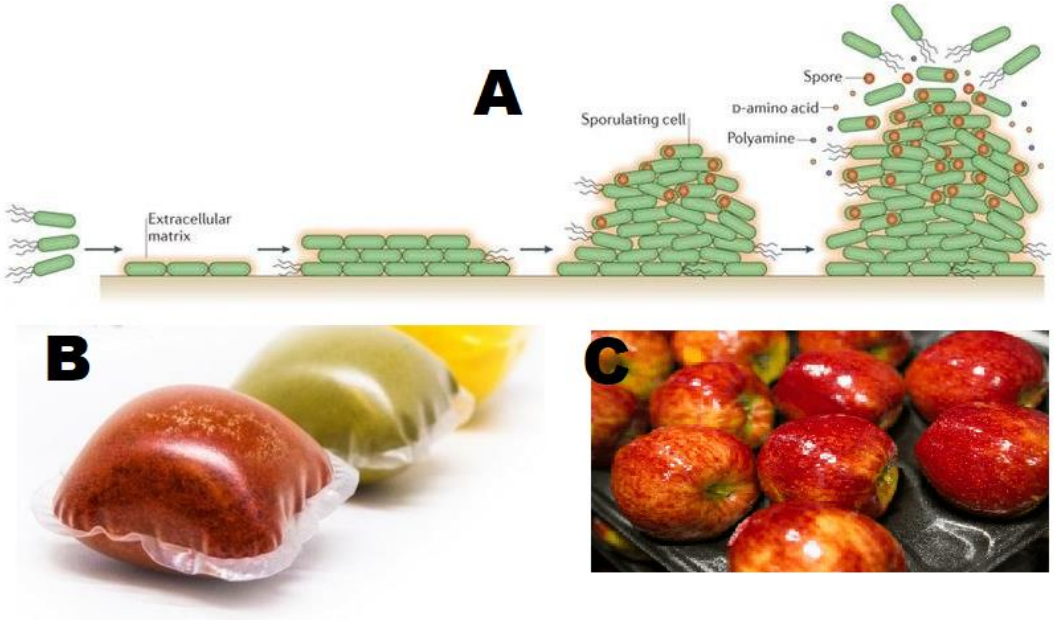

Figure 2 Example of a **(A)** biofilm, **(B)** edible film and **(C)** edible coating.

The main requirement for the consumer is to get high quality products with no preservatives, packed in materials that have practically no environmental impact involved. Consequently, biopolymers that have high compatibility with the intrinsic properties of antimicrobial agents have emerged as one of the most promising active packaging systems (Kuorwel et al., 2011). The main biopolymers used in the formulation of edible films/coatings are proteins from animal or vegetal origin such as wheat gluten, gelatin, soybean proteins, corn

zein, whey, keratin and casein; and polysaccharides, such as cellulose derivates, starches, pectins, alginates, carrageenans, chitosans, fibers and gums. Both groups present superb barrier properties against oxygen, average mechanical properties but high-water vapor permeability (WVP). Composite films can be created by blending proteins and polysaccharides with the aim of achieving optimal properties from each component while minimizing their individual disadvantages (Salgado *et al*., 2015). Currently, there is a special interest in using biopolymers extracted from renewable agricultural resources or industrial by-products, due to its high availability, low cost, and the possibility of adding more value to them. Brewer's spent yeast is an industrial by-product of the beer industry with increased value due the high contents of proteins and polysaccharides that can be extracted from it.

The desired characteristic of the edible films and coatings used in food packaging is the safely and effectively functionality during the required time (shelf-life of the product) and biodegradation capacity. Biodegradability means that these materials can be completely degraded by microorganisms in a composting process, which results in carbon dioxide, water, methane, and some biomass residues as products (Salgado *et al*., 2015). Only water or ethanol are used as solvent during the processing to maintain edibility, and other substances can be added into the materials matrix to improve its functionality. These additives include: *i)* additives that improve or modify the basic functionality of the material, such as plasticizers (mainly polyols - like glycerol, propylene glycol, sorbitol, sucrose, polyethylene glycol -, fatty acids and monoglycerides), cross-linking agents (e.g. transglutaminase or genipin for proteins and citric or tannic acid for polysaccharides), reinforcements (such as fibers, cellulose nanofibers, starch nanocrystals, and chitosan nanowhiskers) for improving mechanical properties, and emulsifiers for stabilization of composite coatings and improvement of its adhesion (e.g. tweens, spans, fatty acid salts and lecithin); *ii)* additives that improve the quality, stability, and safety of packaged foods, such as antioxidants, antimicrobial compounds, nutraceuticals, flavors, and color agents (Salgado *et al*., 2015). Since edible films and coatings may be considered both packaging and food components, they have to fulfill some specific requirements: *a)* good sensory attributes, *b)* high barrier and mechanical properties, *c)* biochemical, physicochemical, and microbial stability, *d)* non-toxicity and safety, *e)* non-polluting nature, *f)* simple technology and *g)* low raw material and processing cost (Salgado *et al*., 2015).

The techniques used into preparing biodegradable films are like the ones used in synthetic polymers. Normally, two main methods of preparation are used: wet processing and

dry processing. Wet processing consists on molding processes that require a solvent (it is the most common technique used to prepare antimicrobial films at a laboratory scale); dry processing involves mainly molding processes through physical procedures such as compression or extrusion of the modified biopolymer if a thermoplastic behavior is required. Therefore, both techniques may alter the final properties of the biodegradable films. There are specific variables that may justify the use of wet processing or dry processing techniques, such as the type of properties that either the biopolymer or the bioactive agent include (e.g. polarity, matrix compatibility), thermal stability of the agent used during processing and finally its residual activity. For instance, when a polar antimicrobial agent is added to a non-polar polymer, the film's physical and mechanical properties may be affected with the inclusion of the agent. However, if the antimicrobial agent is highly compatible with the polymer, it is possible to add a considerable amount to the material with minimal degradation of physical and mechanical properties. So, there will be cases where it will be required to modify some antimicrobial agent properties prior to processing, as it will increase compatibility between the agent and the matrix. It is also mandatory to carefully consider the temperature and shear stresses that will occur during processing. High temperatures may result in considerable losses of volatile bioactive (e.g. antimicrobial) agents. Some studies indicate that the agent may lose partial or even total activity, when inserted in the film under severe processing conditions. Thus, to minimize losses of bioactive agents it is recommendable to apply low temperatures in the film processing as much as possible (Kuorwel *et al.*, 2011).

2 Overview of the main film forming properties

Edible films and coatings must be highly functional according to the product intended to preserve. As such, film forming properties need to be comprehensively studied. A general view related to the properties of an edible film can be described as follows (Han, 2005):

- Edibility and biodegradability – All film components must be natural ingredients and biodegradable (environmentally safe);

- Physical and mechanical protection – An optimization of mechanical properties must be made regarding parameters such as tensile strength, elongation-at-break, modulus of elasticity, compressive strength, puncture strength, stiffness, tearing strength, abrasion resistance, adhesion force, folding endurance, etc.;

- Migration, permeation and barrier functions – Film composition and environmental conditions (relative humidity and temperature) will affect all barrier properties;

- Convenience and quality preservation – An ideal edible film should retard surface dehydration, moisture absorption, oxidation of ingredients, loss of aroma, ageing and microbial contamination of food products. They can contribute to visual quality, surface smoothness, flavor carriage and other marketing-related quality factors;

- Shelf-life extension and safety improvement – Increasing protective functions of food products will extend shelf-life and reduce the possibility of contamination by pathogens.

It is also possible to differentiate numerous activities of an edible film, mainly into two groups: physical-mechanical activities and biological/chemical (biochemical) activities.

Figure 3 shows the general classification proposed.

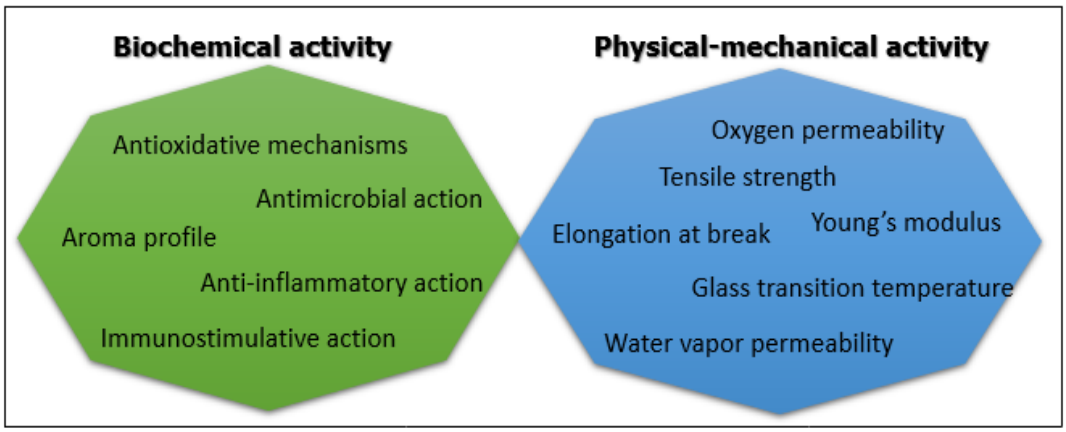

Figure 3 Suggested classification of the different biochemical and physical-chemical properties of an edible film/coating.

2.1 Antimicrobial activity

Impregnating a film with antimicrobial agents is a viable method to achieve an optimal antimicrobial activity. This method allows the gradual release of the agent onto the food surface and an adequate maintenance of agent concentration to effectively inhibit pathogen growth during the shelf life period of the product. This method also allows the agent to be evenly distributed in all the regions of the food surface (Kuorwel *et al*., 2011).

The incorporation of different antimicrobial agents is essential not only to study the behavior of pathogenic cultures, but also to evaluate the agent's effectiveness. For example, several chitosan-based films were developed containing 0.4-2% (v/v) of cinnamon essential oils, being evaluated its efficiency when in contact with pathogens such as *L. monocytogenes*, *L. plantarum*, *E. coli*, *L. sakei* and *P. fluorescens*. It was reported that in agar media, the bacterial growth of all these species was successfully inhibited. Another study used the same matrix (chitosan) but used nisin as the antimicrobial agent. In this situation, the film did not present any inhibitory effect against *E. coli*, showing that the correct choice of the antimicrobial agent is essential when formulating an antimicrobial film (Kuorwel *et al*., 2011).

Proteins can also be used onto film production, having adequate physical and chemical properties. Plant-based proteins are generally used, such as corn gluten, wheat gluten, oat protein, soy protein, among others (Kuorwel *et al*., 2011). Using oat protein incorporated with antimicrobial agents such as nisin, natamycin and malic acid showed great inhibitory growth effect against *P. aeruginosa*, *L. monocytogenes*, *Y. lipolytica*, *P. roqueforti* and *P. commune*. Another study refers the isolated implementation of lauric acid, nisin and EDTA

(Ethylenediaminetetraacetic acid) in a corn gluten matrix, being observed a significative reduction of *L. monocytogenes* growth. However, the same was not verified when EDTA was incorporated (Kuorwel *et al*., 2011).

The right choice of the antimicrobial agent is essential. Other secondary factors, such as concentration and the possible combination with other antimicrobial agents, are important not only to improve film properties, but also to combat a larger pathogenic population. Table 1 shows some examples of incorporated antimicrobial agents in biodegradable polymers.

Table 1 Antimicrobial agents' activity in some packaging materials **[adapted from Kuorwel *et al*., 2011]**.

Packaging material	Antimicrobial agent	Concentration	Microorganism(s)	Observation	Reference
Soy protein /Corn gluten	EDTA	15-30 mM	*L. plantarum*, *E. Coli*	Inhibited *E. coli* at 30 mM	Padgett *et al*. (1998, 2000)
Soy protein /Corn gluten	Lauric acid	2.5-133 mg/g film	*L. plantarum*, *E. Coli*	Inhibited *L. plantarum*	Padgett *et al*. (1998, 2000)
Soy protein/Corn gluten	Nisin	15-30 mM	*L. plantarum*, *E. Coli*	Inhibited *E. coli* at 30 mM	Padgett *et al*. (1998, 2000)
Whey protein	Malic acid	3% (m/v)	*L. monocytogenes*, *P. aeruginosa*, *P. commune*, *P. roqueforti*, *Y. lipolytica*	Inhibited *L. monocytogenes* and *P. aeruginosa*	Pintado *et al*. (2010)
Whey protein	Natamycin	0.002-0.005 g/mL	*L. monocytogenes*, *P. aeruginosa*, *P. commune*, *P. roqueforti*, *Y. lipolytica*	Inhibited *Y. lipolytica*	Pintado *et al*. (2010)
Whey protein	Nisin	50 IU/mL	*L. monocytogenes*, *P. aeruginosa*, *P. commune*, *P. roqueforti*, *Y. lipolytica*	Inhibited *L. monocytogenes*	Pintado *et al*. (2010)

2.2 Antioxidant activity

Antioxidants are molecules that inhibit the oxidation of cellular constituents. The oxidation reactions release the free radicals that may damage cells (Nimse & Pal, 2015) or in this topic of study, the structure of the film. In the food context, some possible measures to avoid the oxidation processes are: *(i)* prevent the oxygen access to the food, *(ii)* use low temperatures, *(iii)* inactivate enzymes that work as a catalyst to oxidation, *(iv)* reduce the oxygen pressure, and *(v)* use of proper packaging. Another method of protection against oxidation is based on using specific oxidative inhibitory additives (antioxidants). These species represent a vast catalog of substances that vary either in chemical structure or action mechanisms (Pokorný *et al*., 2001). Some of these action mechanisms are briefly explained on Table 2.

Table 2 Antioxidative activity mechanisms **(Pokorný *et al*., 2001)**.

Antioxidant class	Antioxidant activity mechanism	Antioxidant examples
Proper antioxidants	Inactivates the lipid free radicals	Phenolic compounds
Hydroperoxide stabilisers	Prevents the decomposition of hydroperoxides into free radicals	Phenolic compounds
Synergists	Promotes the activity of proper antioxidants	Citric acid, ascorbic acid
Metal chelators	Binds heavy metals into inactive compounds	Phosphoric acid, Maillard compounds, citric acid
Singlet oxygen quenchers	Transformes singlet oxygen into triplet oxygen	Carotenes
Substances reducing hydroperoxides	Reduces hydroperoxides in a non-radical way	Proteins, amino acids

The amino acids have a special antioxidant action in protein and polysaccharide-based films, such as films based on proteins and β-glucans that are derived from yeast cultures. Due to its composition being mainly polysaccharides and proteins, the antioxidant agent is already in the matrix. The amino acids can convert the hydroperoxides to imines or, when sulfur is present, to inactive hydroxide groups. Some of the most known reactions of these amino acids, as well as their reaction product are shown on Table 3.

Table 3 Typical amino acid reactions with hydroperoxides **(Pokorný *et al*., 2001)**.

Group	Formula	Reaction Product	Formula
Primary amine	R – NH_2	Imine	= N – R
Secondary amine	R – N – R	Imine oxide	- NR_2 = O
Thiol	R – SH	Dissulphide	R – S – S – R
Dissulphide	R – S – S – R	Thiossulphinate	R – S – SO – R
Sulphide	R – S – CH_3	Sulphoxide	R – SO – CH_3
Selenide	R – Se – CH_3	Selenoxide	R – SeO – CH_3

It would be extremely effective to add pure amino acids onto the film, however, this method is quite expensive. It would be desirable to work with protein hydrolysates because not only they have free amino acids, but also contain peptides, phenolic acids, salts, and other compounds with great antioxidant potential. Thus, the spectrum of the antioxidant action is greatly improved. The hydrolysate can be obtained from inexpensive protein hydrolysis, such as keratin, oat gluten, soy protein, intracellular proteins from brewer's yeast, among many other possible sources. To each food product and existing antioxidants, it is necessary to define which method will be used to verify the antioxidant activity (Pokórny *et al*., 2001). Some examples of incorporated *β*-glucans and mannoproteins as antioxidant agents are given in Table 4.

Table 4 Antioxidant activity of *β*-glucans and mannoproteins found in recent studies.

Antioxidant	Observations	Reference
β-glucan	A positive correlation was observed between the content of *β*-glucans in covered oat grains and the reactive radicals scavenging activity.	Brindzová *et al*. (2008)
β-glucan	The hydroxyl scavenging activity of *β*-glucan was significantly higher than that of various polymers that are used as food additives.	Kofuji *et al*. (2012)
Glucomannan (mannoprotein derivate)	The glucomannan coating incorporated with pineapple core extract was effective in retarding browning.	Supapvanich *et al*. (2012)
β-glucan + mannoprotein supernatant	Mannoproteins and soluble glucans showed a strong scavenging activity. This effect is caused by the protein content of the two supernatants.	Jaehrig *et al*. (2007)

2.3 Anti-inflammatory activity

Some substances possess an anti-inflammatory effect which may help to diminish gastrointestinal tract disorders that have inflammatory characteristics, such as Chronic inflammatory bowel diseases (e.g. Crohn's disease) and ulcerative colitis. The anti-inflammatory action is usually measured by counting the blood leucocytes present in the body (usually lymphocytes T, Tc and B, and granulocytes); these compounds are usually named as peripheral blood mononuclear cells (PBMC) (Suchecka *et al*., 2015). Under an healthy condition, the intestinal immune system produces a healthy mucosa with incidence of a "physiological" inflammation (normal response that prevents injury through its ability to adapt to proinflammatory challenges), otherwise dysregulation of the balance will promote a pathological inflammation (occurrence of an acute infection that usually requires medicine to heal) (Fiocchi, 2008).

Pathogens like lipopolysaccharides (LPS) are endotoxins found in Gram-negative bacteria. When LPS is identified by the immune system, a systemic inflammatory response is initiated, resulting in secretion of cytokine proteins into the blood stream, which in return affects the cells' recognition of compounds considered intruders (Fiocchi, 2008).

Several studies confirm the beneficial effects of β-glucans as anti-inflammatory agents. β-glucans possess the free radical scavenging activity and ability to soothe inflammatory disorders. It is also believed that different physical and chemical properties of β-glucans with distinct molecular weights have different anti-inflammatory effectiveness on organisms. For instance, Suchecka *et al*. (2015) evaluated the effect of a supplemented diet with β-glucans in LPS-induced inflammatory state (enteritis) animals; some results are shown in

Figure 4. G1 represents groups with a diet of β-glucans with high molecular weight, G2 are groups with a diet of β-glucans with low molecular weight, and C represents the initial control groups.

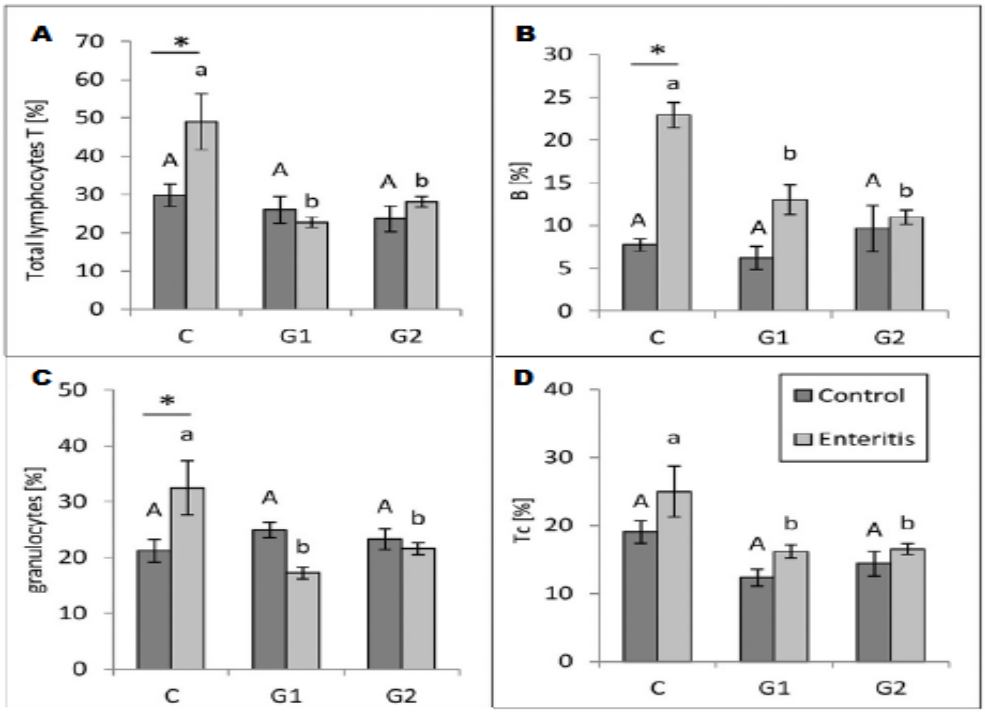

Figure 4 Phenotypic analysis of the isolated PBMC: **(A)** total lymphocytes T; **(B)** lymphocytes B; **(C)** granulocytes; **(D)** lymphocytes Tc. **(Suchecka *et al*., 2015).** Different letters indicate deviation between different groups. Capital letters indicates deviation between the control groups CC, CG1 and CG2. Small letters indicates deviation between enteritis groups EC, EG1 and EG2.

Figure 4 suggests that LPS-induced inflammatory state (enteritis) leads to an increased number of lymphocytes T, B, Tc, and granulocytes, compared with the healthy control group. Between all the control groups, feeding them with *β*-glucans supplementation did not have any correlative impact on PBMC. However, the same does not apply to animals with enteritis. In all scenarios, the PBMC levels decreased greatly, whether the supplementation was from *β*-glucans of low molecular weight or *β*-glucans of high molecular weight. That proves that *β*-glucans can act as anti-inflammatory agents.

Posadas *et al*., (2010) work showed that mannoproteins have an anti-inflammatory action. Rats were subjected to a diet that included several dosages of mannoprotein. An inflammatory cytokine response was induced and a clear action by mannoproteins in cytokine proteins was observed, with lower levels showing up in rats subjected to the mannoprotein diet, compared to higher levels in the control group. It was concluded that mannoprotein administration on a diet appears to protect intestinal tissue against *Salmonella typhimurium* infection. A lower pro-inflammatory response was observed, as well as an inhibition of

apoptosis in cells. However, the regulatory mechanism of anti-inflammatory phenomena remains unknown.

The current anti-inflammatory studies appear to focus mainly in *β*-glucans. A particular study was found that used a *β*-glucan-mannoprotein complex as an anti-inflammatory agent. Apart from the mannoprotein study mentioned above, it seems that there is no additional investigation made regarding isolated mannoprotein as an anti-inflammatory-agent. Further investigation is recommended to evaluate mannoprotein efficiency as an anti-inflammatory agent. Table 5 shows some of the recent studies focused on the *β*-glucans and mannoproteins anti-inflammatory effects.

Table 5 Recent studies of *β*-glucans and mannoproteins as anti-inflammatory agents.

Compound	Observations	Reference
β-glucan	*β*-glucan ingestion attenuated the enhanced concentrations of pro-inflammatory cytokines and increased anti-inflammatory cytokine levels.	Luo *et al*. (2020)
β-glucan	Yeast *β*-1,3-glucan may alter the Th1/Th2 cytokines balance towards a Th2-dependent response by promoting the secretion of anti-inflammatory cytokines.	Chen *et al*. (2013)
β-glucan	Yeast *β*-1,3-glucan recovered the imbalance between the pro- and anti-inflammatory cytokines, showing its anti-inflammatory effect.	Cao *et al*. (2018)
β-glucan + Mannoprotein	*β*-glucan+mannoprotein group decreased the expression of the inflammatory cytokine IL-6.	Johnson *et al*. (2020)

2.4 Mechanical properties

The most important mechanical properties of a film are the elongation (given by a deforming percentage), the resistance to traction (tension) and the Young's modulus, which is inherent to hardness and resistance to fracture (fissure propagation, or cracking). Adding plasticizers onto the film is a necessary requirement to overcome its natural frailty caused by intermolecular tensions. Plasticizers such as glycerol reduce the action of these forces, improving the flexibility and extensibility of the film (Peltzer *et al*., 2018).

The polymer's mechanical properties are influenced by the applied force and temperature. By applying low tensional forces, the polymer's deformation is mainly elastic, *i.e.*, the deformation is homogeneous and after releasing the applied force, the polymer will return

to its original shape and size. On this case, the tensile stress (σ) is proportional to the fractional extension or strain (ε):

$$\sigma = E * \varepsilon \qquad \text{(Eq. 1)}$$

where E is the Young's modulus (or modulus of elasticity) of the polymer, which is a good parameter that describes the material's stiffness. This equation obeys to the Hooke's law, that explains that when a specimen is subjected to a constant deformation rate, the applied tensile strength is directly proportional to the deformation (or elongation) verified. The point in which the applied tension and the deformation are proportionally related is named proportional limit. If the material has forces being applied upon its elastic limit, it will not return to its original shape and size, *i.e.*, a permanent deformation occurs. If the applied forces keep getting higher, the material will start to yield; this point is called yield point, where an increase of applied force does not verify an increment of deformation of the material.

Figure 5 shows the several existent classes of polymers (Polymer Database, 2020).

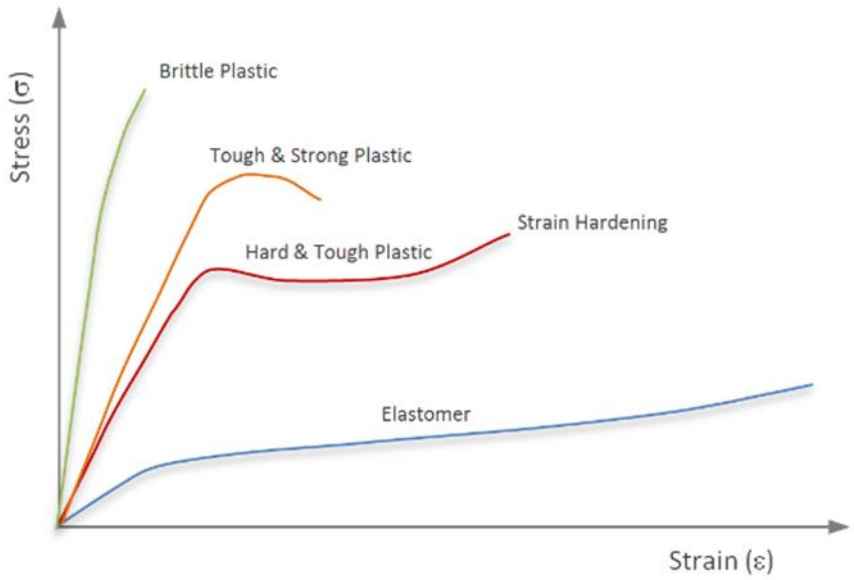

Figure 5 Classification of polymers based on its mechanical behavior when different tensile stresses are applied **(Polymer Database, 2020)**.

2.5 Thermal properties and thermal stability

Thermal analysis is commonly used to study the temperature limits supported by the film. Normally, three types of temperatures are considered: glass transition temperature (T_g), crystallization temperature and degradation temperature. T_g defines the thermal region where the mechanical properties of the material are altered and the hard and brittle state (*i.e.*, "glassy") changes to viscous and deformable, similar to the behavior of rubber (Mettler Toledo, 2020). The crystallization temperature is the thermal point in which the material solidification occurs in a structured form, where the atoms and molecules that constitute the material are highly organized, giving the crystalline attribute to the polymer. Crystallization is accompanied by a certain amount of released energy (exothermic process), which is known as crystallization enthalpy. In addition, the crystallization process is accompanied by a kinetic variable (crystal growth ratio) that must be considered (Netzsch Thermal Analysis, 2020). The thermal degradation temperature is the polymer's service temperature limit in which the material begins to decompose at a molecular level, due to overheating.

There are four conventional techniques used to analyze the thermal properties of biopolymers: DSC (differential scanning calorimetry), TGA (thermogravimetric analysis), TMA (thermomechanical analysis) and the DMA (dynamic mechanical analysis) (Mettler Toledo, 2020). DSC is probably the most used technique since it is possible to obtain the most important parameters that originate from the applied temperature onto the material, such as glass transition zone, melting point, enthalpic and kinetic reactions, as well as the effect caused by additives or plasticizers. TGA consists in the qualitative analysis of compounds and thermal stability analysis of the material. TMA studies mainly the shrinkage or expansion of materials. Finally, DMA is the method of choice to verify the mechanical behavior of materials, characterizing the dependence of frequencies, tensions, and applied amplitudes onto the material (Mettler Toledo, 2020). DSC and TGA methodologies are described in detail in sub-chapters A and B (Supplementary Material).

2.6 Water permeability properties

Biodegradable films may reduce the water permeability between the food and the environment. Water solubility influences the permeability properties of the film; increased water content in the film increases its elongation, accompanied by a decrease in tensional force and modulus of elasticity. Thus, it is imperative to correctly characterize the film's matrix

hydration level through water retention kinetics and sorption isotherms (Delgado *et al*., 2016). Both concepts and kinetic deductions of the main used equations are described in sub-chapter C (Supplementary Material).

The polysaccharides and the proteins interact strongly with water, which means that any film based on these biopolymers will be classified as hydrophilic polymers. In this context, it is expected that films based in proteins and β-glucans, extracted from brewer's spent yeast, will present hydrophilic properties (Delgado *et al*., 2018).

2.7 Oxygen permeability properties

The oxygen permeability (OP) is one of the most studied properties of films. The equipment used to measure the oxygen permeability is the Oxygen Permeation Analyzer (OPA). The oxygen's molecular diameter (O_2) is 2.98x 10^{-8} cm; therefore, films that contain larger pores may be easily permeated by oxygen. The oxygen barrier is quantified by an oxygen permeability coefficient (OPC), that indicates the oxygen quantity that permeates the surface, per area unit of the packaging material and per unit of time (kg m/ [m^2 s Pa]):

$$\mathrm{OPC} = \frac{\mathrm{OTR} * \mathrm{l}}{\Delta \mathrm{P}} \qquad \text{(Eq. 2.2)}$$

in which the oxygen transmission rate (OTR) can be expressed in cm^3/m^2 s, l is the film's length and ΔP represents the pressure difference. Usually, the oxygen permeability variation between polymeric films occur due to different crystallinity degrees of the matrix, different densities of cohesion energies, amount of free volume in the film, etc. Protein films possess a great oxygen barrier compared to non-ionic polysaccharidic films due to the high polarity of the protein and linear structure (no ring-shaped structure). The film's testing variables, like temperature and relative humidity, will greatly change its permeability (Jawaid *et al*., 2018). An experimental procedure is described in sub-chapter D (Supplementary Material).

2.8 Plasticizers

Edible films are derived from renewable sources such as polysaccharides, lipids, and proteins. Among these materials, proteins present higher ability to form films with better mechanical and barrier properties than polysaccharides; however, protein-based films are very

brittle. Therefore, plasticizers are added to edible films to reduce chains interactions which stabilizes the film network, resulting in the increased mobility of molecules. Nevertheless, plasticizers generally cause an increment on the gas and water vapor permeability of films. Thus, plasticizers must be added at a certain amount to obtain films with improved flexibility without significant decrease of barrier properties to mass transfer (Jongjareonrak *et al*., 2006).

Hydrophilic plasticizers, such as glycerol, polyethylene glycol and sorbitol are largely used in edible films to improve mechanical properties. However, the differences in composition, size, structure, and shape of plasticizers directly influence their ability to function in the film network (Jongjareonrak *et al*., 2006). Bourtoom *et al*. (2006) evaluated the mechanical properties of a film based on water-soluble fish proteins using different plasticizers (sorbitol, glycerol, and polyethylene glycol). Results showed that sorbitol plasticized films were the most brittle but showed the highest tensile strength. However, the effect on the water vapor permeability was low. In contrast, glycerol and polyethylene glycol plasticized films presented structural flexibility with low values of tensile strength which resulted in a higher water vapor permeability. When plasticizer concentration increased, the tensile strength decreased associated with an increase in the elongation at break and higher water vapor permeability. Sorbitol plasticized films showed higher film solubility and protein solubility, compared to glycerol and polyethylene glycol plasticized films. Overall, an increment in the plasticizer concentration resulted in higher film and protein solubility. The color of the films was more affected by the type of plasticizer used than its concentration (Bourtoom *et al*., 2006).

Currently, there is no available research regarding the plasticization effects on *β*-glucan, mannoprotein and *β*-glucan-mannoprotein edible films. However, there are some investigations that studied the plasticizing effects on yeast cell wall-based films, which should contain considerable amounts of *β*-glucans and mannoproteins. Table 6 shows the main findings regarding these films.

Table 6 Plasticizing effects on yeast-based films.

Matrix	Plasticizer	Conclusions	Reference
Residual yeast cell wall	Glycerol (from 0 to 35% w/w)	Enhanced solubility; Young's modulus and tensile strength decreased; 15% glycerol presented the best properties.	Peltzer *et al*. (2018)
Yeast biomass	Glycerol (from 0 to 30%)	Increased glycerol content leads to higher water solubility and permeability; higher film thickness led to lower water solubility and higher diffusion.	Delgado *et al*. (2018)

3 *β*-glucans and mannoproteins from *Saccharomyces cerevisiae*

3.1 *S. cerevisiae*

The conventional brewing process has a long history, being started 8000 years ago. Despite being considered a pioneer process of traditional biotechnology, this industry is still a dynamic one that is constantly improved and modified, according to the contemporary requirements of the market. Fundamentally, beer is the product from the alcoholic fermentation of malted cereals by yeasts of *Saccharomyces cerevisiae* genre. The use of different cereals or different temperature/ time conditions are crucial parameters and allow distinct beer profiles (Ullrich, 2011). Data from 2018 indicate a worldwide beer production of 191.1 hm^3 (cubic hectometers) and the main beer producers were China, USA, and Brazil, with 20.4, 11.2 and 7.4% of the market share, respectively (Kirin Holdings, 2019).

The beer industry generates large amounts of by-products, such as brewer's spent grains, brewer´s spent yeast, spent hops, and fermentation reaction products (carbon dioxide and ethanol). Brewer´s spent yeast is the second largest by-product from the brewing process. It is estimated that for each kilogram of initial yeast used for the fermentation process, 4 to 5 kilograms of yeast are generated, explaining the amount of exceeding yeast considered as a by-product (Feedipedia, 2018). From another point of view, for each liter of beer produced, around 2 grams of exceeding yeast are generated. This exceeding yeast can still be reused in the process and depending on the fermentation conditions and the yeast's species, it can last through 4 to 12 fermentative cycles. However, when yeast biomass presents inadequate viability and vitality properties, which are essential for the fermentation step, it is disposed from the brewing process and considered a by-product (Stewart *et al.*, 2017).

3.2 *S. cerevisiae* cell structure

The *S. cerevisiae* cell structure is shown in

Figure 6. The proteins and the polysaccharides found in the cell wall (dry weight) are mostly represented by *β*-glucans (55-65%; with chitin representing 1-2%) and mannoproteins (35-40%) (Klis *et al*, 2002).

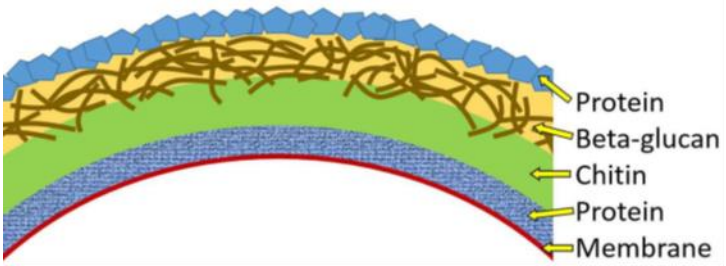

Figure 6 Scheme of a *S. cerevisiae* yeast cell wall **(adapted from Action International, 2019).**

3.2.1 *β*-glucans

The cell wall's internal layer contains glucans, mostly *β*-(1-3)-glucan (85%) and *β*-(1-6)-glucan (15%), Figure 7. The main chain of the molecule is composed of *β*-(1-3)-type linkages and on the ramifications, *β*-(1-6)-type linkages are predominant. There is a covalent bond between these glucans and the external layer's mannoproteins. There is also a residual amount of α-(1-4)-glucan covalently bonded to *β*-(1-6)-glucan (Bastos *et al.*, 2015).

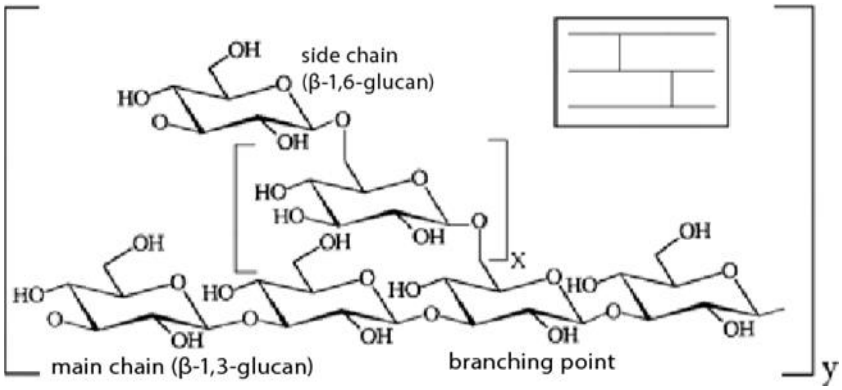

Figure 7 Molecular structure of a *β*-glucan **(Zechner-Krpan *et al.*, 2009)**.

From literature search, it is possible to understand that *β*-glucan is a substance that can be easily modified physically or chemically to obtain specific desired properties. Some of the properties are described in a review article by Kaur *et al.* (2020) and a short conclusion of the many investigations referred in that research is shown in Table 7 Properties of *β-glucans* found in several investigations..

Table 7 Properties of *β*-glucans found in several investigations.

Property	Observations	Reference
Great hydrophilicity	Large quantities of water are absorbed by barley and oat *β*-glucan rich extractions.	Tejinder *et al*. (2000)
Stabilizer	Sonication is successfully used to avoid agglomeration and to improve the stability of the *β*-glucan suspension.	Zechner-Krpan *et al*. (2010)
Thickener	Its ability to trap a large amount of water and intrinsic rheological characteristics make β-glucan an ideal thickener	Methacanon *et al*. (2011)
Health benefits	β-glucans can stimulate both innate and adaptive immune responses and could be used for cancer immunotherapy treatment.	Chen & Seviour (2007)
High solubility range	*β*-glucan extracted from different sources of cereals has a wide range of molecular weights and modified solubility.	Tosh *et al*. (2010)

3.2.2 Mannoproteins

Mannoproteins are found on the exterior surface of the cell wall and include the *N*-mannans if the chiral carbon is connected to a nitrogen from an asparagine or arginine; and the *O*-mannans if they form a glycosidic bond with the oxygen from the hydroxyl group of a serine or threonine molecule. A simplified depiction of these two types of mannans is shown in Figure 8. *N*-mannans are the main mannoproteins found in the fermentative process, having between 50 to 200 units of α-(1-6), α-(1-2) and α-(1-3)-mannose. They are made of 90% carbohydrates and 10% proteins, being important for the structural function of the cell wall. They can also contain residual mannosylphosphate groups that contribute to ionic properties of the cell's surface. *O*-mannans are made of 50% protein and 50% carbohydrates, having oligosaccharide chains between 1 to 5 α-(1-2) and α-(1-3)-mannose units, and usually containing one mannosylphosphate unit. These types of proteins control the enzymatic activity (Bastos *et al*., 2015). Some interesting properties of mannoproteins are shown in Table 8.

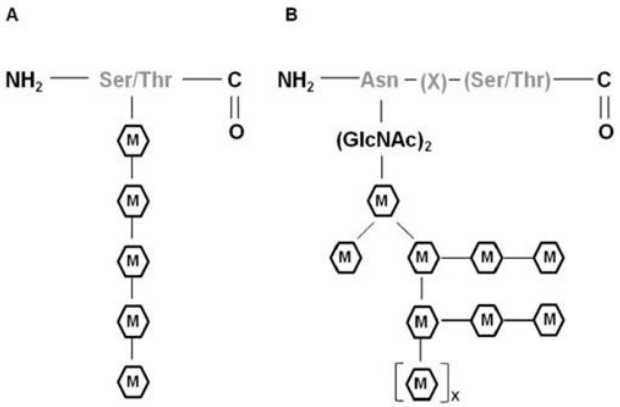

Figure 8 Structures of **(A)** *O*-mannans and **(B)** *N*-mannans **(Blasco *et al*., 2011).**

Legend: Ser/Thr – Serine/Threonine; GlcNAc – N-acetylglucosamine; Asn – Asparagine; X – aminoacid; M – mannose.

Table 8 Properties of mannoproteins found in recent investigations.

Property	Observations	Reference
Emulsion activity	Similar emulsifying properties compared to conventional food emulsifiers (e.g. gum arabic, lecithin)	Dikit *et al*. (2010)
Antifungal activity	Reduction of *Aspergillus flavus* growth and consequent reduction of aflatoxins	Abdolshahi *et al*. (2016)
Barrier properties	Directly influence permeability such as oxygen or water vapor permeability	Zimkus & Chaustova (2003)

3.3 Isolation and characterization of *β*-glucans from *S. cerevisiae* yeast cell wall

The application of different extraction methods has a direct influence on the permeability and foam formation of *β*-glucans. Literature refers an inverse relation between the viscosity and the foam formation, but a direct relation between the viscosity and the solubility of *β*-glucans (Zhu *et al*. 2015). A study showed that the cell walls of homogeneous yeasts (cell wall's size reduction at a microscopical level) exhibit a larger content of *β*-glucan and a higher apparent viscosity compared to non-homogeneous yeasts. The homogenization procedure promotes a more effective cell wall fragmentation and therefore, a higher extraction of *β*-glucans. It was also concluded that in homogeneous yeasts, the obtained *β*-glucan possessed a larger ability to retain water and a higher stability in an emulsion state (Thammakiti *et al*., 2004).

Despite the cheap price of raw material used to extract glucans, the processes of extraction and purification of *β*-glucans usually imply huge costs and may contribute to polysaccharide degradation (Peltzer *et al*., 2018). Therefore, using purified *β*-glucan to formulate an edible film is not economically viable. Thus, if a separation method does not impose a high glucan purity level, some proteins may remain bonded to the polysaccharide and the formulation of an heterogeneous dispersion may be achieved. This will be useful for applications and/or materials that demand specific properties of both proteins and polysaccharides, as is the case of films/coatings (Zhu *et al*., 2015). On the other hand, the molecular weight of *β*-glucan depends on the aggregation and depolymerization phenomena that occurs during the extractive process. Therefore, the most appropriate extraction method will directly depend on the source and structural characteristics of the *β*-glucan. However, it is crucial to take into consideration that some extraction methods show major disadvantages, such as high extraction time, high processing costs and increased environmental impact. Then, it is necessary to make a precise analysis on the method to use and whether it is really required to obtain a *β*-glucan extract of high purity (Zhu *et al*., 2015).

Shokri *et al*. (2008) applied a conventional method of extraction and isolation of *β*-glucans, with a subsequent purification technique. In this protocol, a pre-treatment is required, where cell walls are disrupted by sonication (ultrasound bath) and with the addition of a phosphate buffer solution. Then, cell walls and intact cells are separated by centrifugation; it is recommended to centrifuge cell walls at temperatures as low as 4 ºC since it will help cell walls to pack faster and to not lose any significant biological activity. After this stage, the cell wall material is submitted to an alkaline extraction by adding a sodium hydroxide solution, at high temperature and time parameters (the study suggests 90 ºC and 5 h). After cooling and centrifuging the extract, the precipitate is discarded, and the supernatant is treated with acetic acid to neutralize the media. The addition of ethanol will precipitate *β*-glucan. This solution is treated with acetic acid and centrifuged to remove any remaining proteins. The supernatant is recovered, neutralized with sodium hydroxide, and lyophilized for future usage (Substrate 1). The extract is still not purified. At this point, the solution contained 2.4% of undiscriminated proteins. Thus, an AEC (anion exchange chromatography) technique is used. The solution is loaded into a DEAE-C (Diethylaminoethyl cellulose) column, which consists of a positive charged resin that will lock negatively charged proteins into its matrix. The *β*-glucan content is then eluted into a Tris-HCl (tris-hydroxymethylaminomethane hydrochloride) buffer at pH 8 (Substrate 2). Then, an affinity chromatography technique is applied to remove mannans from

the solution. The concanavalin-A resin captures glycosylated molecules such as glycoproteins and glycolipids, with a strong affinity for α-D-mannose. The *β*-glucan is then collected by elution in Tris-HCl buffer at pH 7.5 (Substrate 3). Table 9 and Table 10 show some important results by using this protocol.

Table 9 Weight parameter of each obtained substrate **[Adapted from Shokri *et al.*, 2008]**.

Analyzing parameter	Product	Weight
Yeast biomass	Yeast cells	19.3 g
Yeast disruption	Cell walls	4.14 g
Alkaline extraction	Substrate 1	1.14 g
DEAE-C chromatography	Substrate 2	2 g
Con-A chromatography	Substrate 3	62.4 mg

Table 10 Yields of biomolecules found in the yeast cell wall **[Adapted from Shokri *et al.*, 2008]**.

Purification step	Protein (% w/w)	*β*-glucan (mg dL^{-1})	Mannan (mg dL^{-1})	Mannan/*β*-glucan ratio (up to 100%)
NaOH extraction	2.41	32.8	77.8	70.3/29.7
DEAE-C chromatography	0.004	21.5	68.5	71.9/28.1
Con-A chromatography	Not detected	14.3	0	0/100

It is possible to conclude that a pure *β*-glucan extract may be achieved, however, the process is not economically feasible at an industrial scale. The mass obtained (62.4 mg) is around 300 times lower compared to the initial mass of the yeast cells (19.3 g), with a *β*-glucan concentration of 0,143 g found in 1 liter of yeast cell wall solution. Proteins are not detected at the final stage because the small amounts that still remain are in the form of mannoprotein complexes that are isolated by binding with concanavalin-A present in the chromatographic column (Shokri *et al.*, 2008). There is also an issue regarding the inherent loss of *β*-glucan throughout the purification steps, as it can be seen by the decreasing concentration tendency in the chromatographic stages. These techniques also use very specific resins which comes associated with high costs not only in the act of purchasing the columns but also maintaining them operational.

3.4 Isolation and characterization of mannoproteins from *S. cerevisiae* yeast cell wall

It is hard to isolate mannoproteins of brewer's spent yeast due to the high heterogeneity of their structures. One of the most used methods is the acid-alkaline method. This process is based on the principle that a material containing comminuted proteins homogenized in water are affected by the pH of the mixture. In a molecular point of view, at severe acid or alkaline conditions, strong changes on the cationic or anionic charge of the cell will drive apart exoskeletal proteins which in return will promote interactions with the surrounding water and therefore, solubilize the proteins. The degree of protein solubility will be influenced by the electrostatic and hydrophobic interactions between protein molecules; when the electrostatic repulsion is higher than hydrophobic interactions, proteins are extracted. At extreme pH conditions, solubility can increase up to five times that of the starting one, which can be explained by the co-extraction of the restraining proteins that cannot be extracted at neutral pH. According to Kristinsson & Hultin (2003), the acid-alkaline extraction can be summarized into three steps:

(a) Homogenization - proteins are added adequate amount of water to keep viscosity at a low level;

(b) pH shifting - the homogenate is solubilized by addition of a base or an acid. The goal is to reach a desired pH that will solubilize proteins;

(c) High-speed centrifugation and separation - the homogenate is centrifuged and the precipitate is separated from the dissolved material. This process aims to separate all non-soluble proteins and some other non-desirable compounds. The separation depends on four main factors: particle size, liquid density, particle density and viscosity (Kristinsson & Hultin, 2003).

Behind acid-alkaline method, other methods have been used to recover mannoproteins from *S. cerevisiae* cell wall, namely, pulsed electric field (PEF), heat treatment, sodium dodecyl sulfate (SDS) and enzymatic treatment. PEF is a nonthermal method that destructs or inactivates microorganisms, which is achieved by breakdown of the microorganism's cell membranes by being exposed to electric fields. Multiple short pulses of high-intensity energies (20-50 kV cm^{-1}) are applied between two electrodes. The treatment is adjusted to the sample's characteristics, varying four parameters: pulse frequency; intensity (kV cm^{-1}) of the electric field; exposure time; and shape of the pulse wave (Graham, 2003). According to Martinez *et al*. (2016) protocol, *S. cerevisiae* biomass was resuspended in a citrate-phosphate buffer and subjected to

PEF at a defined frequency and intensity. Cells were placed in a potato-dextrose-agar media to monitor inactivation and the mannoproteins release was monitored by determining the mannose concentration of the supernatant after hydrolyzation (adding sulfuric acid). As observed in **Error! Reference source not found.**, the mannose concentration into the extracellular environment was increased drastically in solutions pre-treated with PEF technique; after 25 days of incubation PEF-treated cells presented a solution with 10 times more mannose than the untreated ones (Martinez *et al*., 2016).

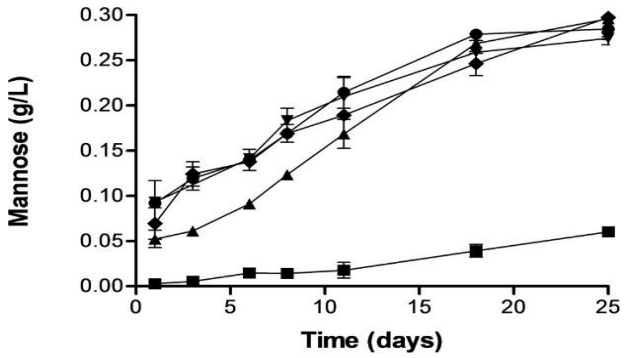

Figure 9 Release of mannose from *S. cerevisiae* cells untreated and treated by PEF treatments of different intensity **(Martinez *et al*., 2016).**

Legend: Untreated (▪), 15 kV/cm 45 μs (▲), 15 kV/cm 150 μs (▼), 25 kV/cm 45 μs (◆), 25 kV/cm 150 μs (●).

The heat treatment can resolubilize soluble macromolecules such as noncovalently bound mannoproteins, by affecting its inter-hydrogen bonds. According to Li *et al*., (2020) procedure, suspensions of brewer's yeasts at a concentration of 5% (w/v) were prepared in a phosphate buffer which stabilized the pH to 7. Then, the suspensions were heated at 90 ºC for 4 hours. After cooling, a centrifugation was made to separate the supernatant from the precipitate, in which the latter was discarded. The supernatant was dialyzed against water to retain a more purified extract of mannoproteins, and then freeze-dried (Li *et al*., 2020). These authors also tested the SDS and the enzymatic treatments. For the SDS treatment, brewer's yeast was suspended in a mixture of SDS reagent and yeast at a concentration of 2% and 5% (w/v), respectively. Then, the solution was incubated at 100 ºC for a period of 5 min, following centrifugation. The supernatant was once again recovered, dialyzed, and freeze-dried (Li *et al*., 2020). A Zymolyase® enzyme kit (β-1,3-glucan laminaripentaohydrolase and β-1,3-glucanase) was used for the enzymatic extraction. The enzyme was added to the suspension of yeast

prepared with the same concentration as the last methods mentioned. A phosphate buffer was once again added to maintain a pH of 7.5, where enzymatic activity is higher. The enzymatic reaction occurred during 4 to 20 hours, at 35 ºC, under 200 rpm agitation. After the reaction time is reached, the reactions were inactivated at 60 ºC for 10 min. The recovered supernatants were freeze-dried and then subjected to an affinity chromatography, where mannoproteins were eluted in an α-D-methylglucoside solution, which was used as the mobile phase. The recovery yields obtained with these three extraction methods are shown in Table 11.

Table 11 Effect of the extraction methods used on the isolation of mannoproteins from brewer's yeast **[adapted from Li *et al.*, 2020]**.

Method	Yield of recovered extract (%)	Protein recovery yield (%)	Mannoproteins recovery yield (%)
Heat treatment	38.5	48.0	40.5
SDS extraction	26.3	35.5	24.7
Enzymatic treatment	31.4	55.8	78.0

Results showed that SDS extraction had a more ineffective approach to extract mannoproteins, with a mannan recovery yield of 24.7% in a recovered extract yield of 26.3%. The best treatments were the heat treatment and the enzymatic treatment (Li *et al.*, 2020). It is hard to define which one is the best because a preliminary study associated with the method cost and its yield should be made, to understand if the highest recovery yield is the priority. If that is the case, then enzymatic treatment may be considered the best method. However, if the extraction does not require high amounts of mannan and optimized yield quantities, then heat treatment can be considered the best method, since it is less expensive.

4 Use of *Saccharomyces cerevisiae* cells as a film forming material

4.1 *S. cerevisiae β*-glucans film forming properties

Literature refers some β-glucans edible films prepared from *S. cerevisiae* (Novák *et al*., 2012, Blahovec *et al*. (2011), Sárossy *et al*. (2012)). Glycerol is generally used as a plasticizer and different physical and chemical properties have been evaluated. The surface properties, degree of crystallinity and ageing effects have been estimated by scanning electron microscopy (SEM), atomic force microscopy (AFM) and X-ray diffraction (XRD). The mechanical properties have been characterized by tensile tests and the thermal properties by DSC. According to Novák *et al*. (2012) study, the β-glucans films showed a partial solubility when immersed in water with a weight loss of around 26%, which corresponded to the amount of glycerol in the film. Within this result, the practical theory that *β*-glucan is insoluble was reinforced. In addition, through XRD analysis it was possible to observe that films were homogenous and transparent. A relative structural disorganization of the surface was observed and attributed to a reorientation and decomposition of surface macromolecules in contact with the atmosphere (Novák *et al*., 2012).

Blahovec *et al*. (2011) evaluated the tensile properties of *β*-glucan films containing 25% of glycerol, with a relative humidity of 43%. From 21 measurements, the final values of modulus of elasticity, yield stress, strength and strain at rupture were 712 ±31 MPa, 9.45±0.37 MPa, 17.48±0.61 MPa and 14.16±1.11 MPa, respectively. It was also concluded that an increment of 4% plasticizer concentration decreased by 50% the original modulus of elasticity and yield stress. The strength of the film decreased linearly by adding plasticizer and tends to zero when plasticizer concentration was around 40%. The strain at rupture increases with increasing concentration of plasticizer. In addition, during long-term storage at a relative humidity of 51%, the elasticity modulus` increased but a a decrease of the strain at the rupture point was observed. Strength also increased linearly with the square root of the modulus of elasticity, which might indicate that crack mechanisms occur in the deformation process (Blahovec *et al*., 2011).

The SEM images show the surface morphology of the film (Figure 10). The morphology reflects the complex interactions within the film, as well as interaction between the film and the atmosphere during its solidification. At a microscopic level, irregularity of the surface can be

attributed to desiccation, non-homogeneity of a suspension containing cell wall fragments or high viscosity in the final stages of relaxation. High magnification pictures show some string-like structures that exceed 10 μm that can be attributed to fiber biopolymers. Films are compact and practically non-porous (Novák *et al.*, 2012).

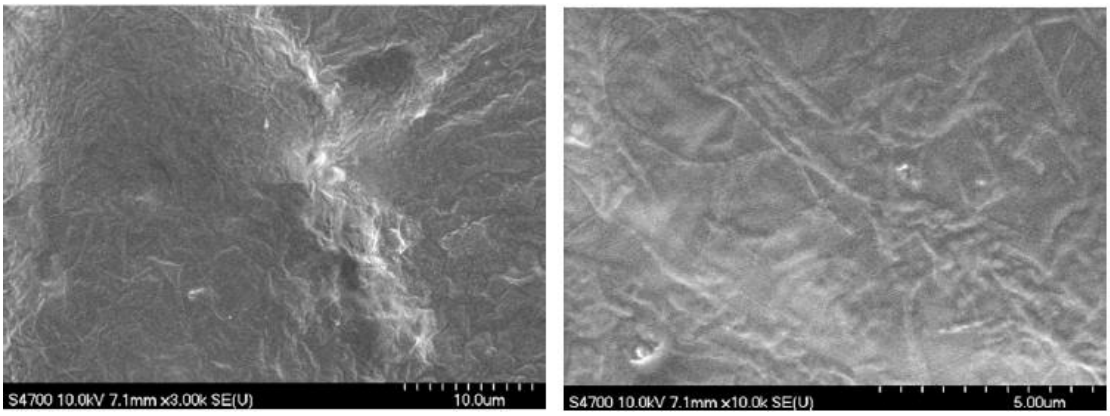

Figure 10 SEM images of the yeast *β*-glucan film, amplified 3000x (left) and 10000x (right) **[Novák *et al.*, 2012]**.

The AFM analysis shows the morphology and roughness of the film (

Figure 11), including the effect of ageing. The first series of measurements was performed right after the film preparation (A) while the second one was just after 12 months (B). In the first case, the surface consisted of granular-like structures. After ageing, protected from direct light and dust deposition in an air-conditioned laboratory (20 ºC), a mild increase of surface roughness was observed, and the characteristic granular structure of the film was gone. The resulting structure consisted of numerous formations which were several hundred micrometers high and up to few micrometers wide (Novák *et al.*, 2012).

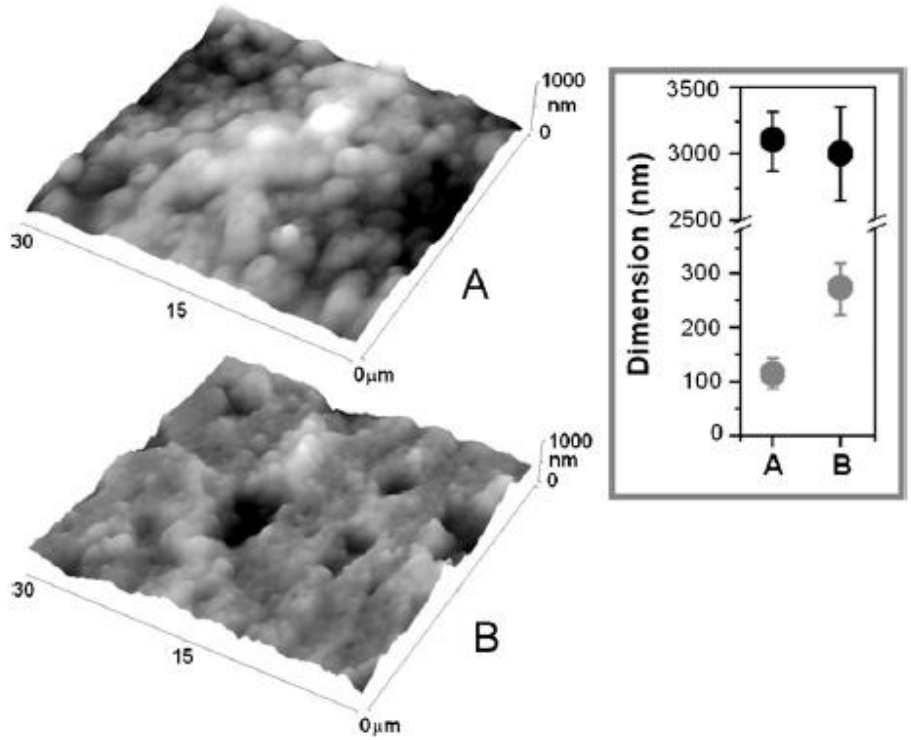

Figure 11 AFM images of the **(A)** yeast *β*-glucan films immediately prepared and **(B)** after 12-month storage (left images). Influence of 12-month storage on the height (black circles) and width (grey circles) of the granular particles in yeast *β*-glucan films according to AFM (right image) **[Novák *et al*., 2012]**.

In conclusion, the produced *β*-glucan film is water insoluble, compact, non-porous, exhibits no pronounced crystallinity. Structurally, it consists of granular-like and fiber microstructures, assigned to cell wall residues and polysaccharides. Some structural changes are verified in the film surface during a one-year shelf storage period, which can be related to reorientation and decomposition of surface macromolecules caused by reactions with the ambient atmosphere.

Sárossy *et al*. (2012) analyzed the effect of adding *β*-glucans into arabinoxylan films. The arabinoxylan films with no *β*-glucan content presented a significant decrease in mechanical properties compared to the arabinoxylan-*β*-glucan blend films. The average tensile strength of the blended film (20% addition of *β*-glucan) was around 32.8 MPa, while the arabinoxylan film showed a tensile strength of 15.7 MPa. Elongation at break also decreased from 10.6% to 6.1%. A lower decrease was observed for the Young's modulus.

Sárossy *et al*. (2012) evaluated the film's water content at different relative humidities (RH). The comparison between pure *β*-glucan films, arabinoxylan films and arabinoxylan-*β*-glucan blende films is presented in Table 12.

Table 12 Water content of pure arabinoxylan and *β*-glucan films, and blend films of arabinoxylan-*β*-glucan with varied mass ratio, at different relative humidities (RH) **[Adapted from Sárossy *et al*., 2012]**.

Film	**Water content (%)**		
	50% RH	**75.5% RH**	**98% RH**
Arabinoxylan	11.9 ± 0.3	13.7 ± 1.3	41.5 ± 0.1
Arabinoxylan- *β*-glucan (80:20)	10.1 ± 0.5	14.4 ± 1.0	38.1 ± 3.7
Arabinoxylan- *β*-glucan (50:50)	11.9 ± 0.6	15.0 ± 1.5	36.5 ± 3.8
Arabinoxylan- *β*-glucan (20:80)	10.9 ± 0.1	14.8 ± 1.0	42.4 ± 2.1
β-glucan	13.4 ± 1.5	15.9 ± 0.3	43.9 ± 0.6

Results from Table 12 showed that at 50, 75.5 and 98% RH, the pure *β*-glucan films presented the highest water content due to a higher water affinity compared to arabinoxylan. The *β*-glucan ratio in blend films appears to not have a direct correlation in the increase of water content. For example, at 50% RH, the ideal amount of *β*-glucan in the blend film with the highest water retention capability appears to be 50% *β*-glucan, since the highest content of *β*-glucan blend film (80%) shows a lower water content. The same scenario is observed at 75.5% RH. However, at 98% RH, the *β*-glucan blend film with the highest content of *β*-glucan showed the highest water content out of the three blend films. According to the authors of the study, arabinoxylans are very hygroscopic and absorb a great amount of water in high humidity environments. Furthermore, *β*-glucan chains form a more compact structure compared to arabinoxylans which can result in lower water absorption of films containing *β*-glucans at high humidities. Therefore, the water content of the *β*-glucan blend films was not influenced greatly at higher RH values. The study concluded that *β*-glucan films had higher water contents between 11 and 75% RH, but the tendency is reversed at 91% RH (Sárossy *et al*., 2012). Other parameters were also assessed in this study; the main results are reported in Table 13.

Table 13 Water vapor transmission rate (WVTR), water vapor permeability (WVP), oxygen transmission rate (OTR) and oxygen permeability (OP) of pure arabinoxylan and *β*-glucan films, and blend films of arabinoxylan-*β*-glucan with varied mass ratio, at approximately 52% relative humidity **[Adapted from Sárossy *et al.*, 2012]**.

Film	WVTR (g/m^2 d)	WVP (g mm/kPa m^2 d)	OTR (ml/m^2 d)	OP (cm^3 mm/m^2 d kPa)
Arabinoxylan	204 ± 1	7.7 ± 0.5	2.32 ± 0.87	0.87 ± 0.24
Arabinoxylan-*β*-glucan (80:20)	224 ± 8	7.9 ± 0.1	2.74	1.30
Arabinoxylan-*β*-glucan (50:50)	293 ± 8	9.9 ± 0.4	3.75	1.60
Arabinoxylan-*β*-glucan (20:80)	283 ± 5	13.0 ± 0.0	7.19 ± 1.79	1.97 ± 0.79
β-glucan	363 ± 8	12.3 ± 1.2	3.91 ± 1.42	1.23 ± 0.72

It is observed that *β*-glucan film samples possessed a significantly higher WVTR compared to the other formulations. This was expected, due to its high-water affinity. It is also observed that, when added to another matrix such as arabinoxylan, it does not reduce the WVP of a blend-type film. In fact, it appears that its addition might improve WVP. It is noticed that the arabinoxylan-*β*-glucan (20:80) film presents a higher value of WVP when compared to the pure *β*-glucan film. This suggests that when the blend proportion is ideal, there might be a larger number of binding sites to form hydrogen bonds in the presence of water (Sárossy *et al*., 2012).

The *β*-glucan film presented high OTR and OP values but the arabinoxylan-*β*-glucan (20:80) film showed improved oxygen permeability properties. The presence of aggregated particles, zones of the film with varied thickness, as well as pinholes might be the major cause of the differences in permeability between the one- and two-component films (Sárossy *et al.*, 2012). The authors concluded that the addition of *β*-glucans does have a positive effect on the mechanical properties of arabinoxylan films. It should be considered that depending on the film matrix used, the conclusions might differ from the ones mentioned in this study. In order to check this possibility, a recent investigation used a pullulan-based film matrix and added *β*-glucans into the formulation (Chang et al., 2019). The authors observed an improvement of mechanical properties when *β*-glucans were added to the film. The results are highlighted in Table 14.

Table 14 Mechanical properties of pure pullulan, *β*-glucan, and pullulan-*β*-glucan blend films. The described ratios consist of the fraction of each component per gram of the film **[adapted from Chang *et al*., 2019]**.

Films	Tensile strength (MPa)	Elongation (%)	Thickness (mm)
Pullulan (PUL1)	7.58 ± 1.04	23.47 ± 2.64	0.042 ± 0.003
Pullulan-*β*-glucan (0.25:0.05) (BP2)	17.00 ± 1.69	38.73 ± 1.65	0.044 ± 0.001
Pullulan-*β*-glucan (0.2:0.1) (BP3)	25.17 ± 2.93	57.27 ± 1.21	0.049 ± 0.001
Pullulan-*β*-glucan (0.15:0.15) (BP4)	33.81 ± 0.67	64.61 ± 7.06	0.051 ± 0.002
Pullulan-*β*-glucan (0.1:0.2) (BP5)	34.62 ± 0.76	75.86 ± 8.30	0.051 ± 0.002
Pullulan-*β*-glucan (0.05:0.25) (BP6)	30.77 ± 0.68	54.72 ± 5.04	0.052 ± 0.003
β-glucan (BG7)	48.44 ± 0.92	79.74 ± 10.67	0.052 ± 0.002

Among all the films tested, the pure *β*-glucan film showed the best mechanical properties. The addition of *β*-glucan proved to increase the tensile strength and elongation of the blend film (Chang et al., 2019). This is suggested to occur due to the formation of hydrogen bonds between pullulan and *β*-glucan. The last pullulan-*β*-glucan film showed a decrease in tensile strength and elongation, probably due to lower pullulan content and a weaker phase separation. The difference of thickness between the tested films was not considered significant; however, as *β*-glucan content increased, the film thickness also increased, showing that the film thickness is dependent on the quantitative and qualitative compositions of the film (Chang *et al*., 2019). The water solubility of the films was also tested, this parameter shows the water resistance of film and influences its applicability as packaging material in products. The results are shown in the **Error! Reference source not found.**.

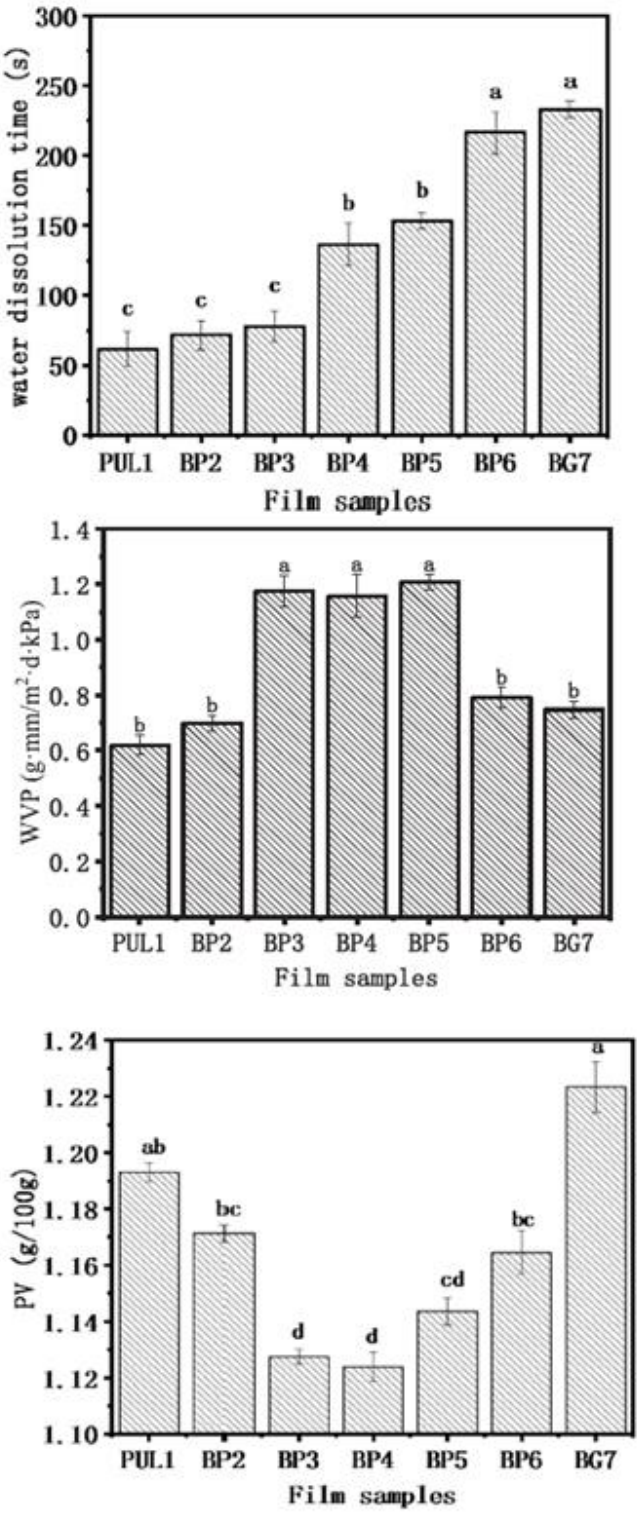

Figure 12 (A) water dissolution time, **(B)** water vapor permeability, and **(C)** oxygen permeability of pullulan film, β-glucan film and blend films **[Chang *et al.*, 2019]**.

Legend: (PUL1) Pullulan; **(BP2)** Pullulan-*β*-glucan (0.25:0.05); **(BP3)** Pullulan-*β*-glucan (0.2:0.1); **(BP4)** Pullulan-*β*-glucan (0.15:0.15); **(BP5)** Pullulan-*β*-glucan (0.1:0.2); **(BP6)** Pullulan-*β*-glucan (0.05:0.25); **(BG7)** *β*-glucan.

Among the blend films, BP2 (pullulan-*β*-glucan = 0.25:0.05) and BP3 (pullulan-*β*-glucan = 0.2:0.1) showed the best solubility, due to a lower dissolution time. By increasing the *β*-glucan content, the water solubility of the blend films decreased. It was suggested that the aggregated chemical structure of the *β*-glucan blend films (with lower solubility) may affect the water absorption (Chang *et al*., 2019).

Chang et al., (2019) also assessed the film's barrier properties, specifically the WVP and OP. Results showed that among all the films tested, the pullulan and *β*-glucan films presented the lowest values of WVP, which in return demonstrates a higher moisture resistance. Among the blend films, BP2 (pullulan-*β*-glucan = 0.25:0.05) and BP6 (pullulan-*β*-glucan = 0.05:0.25) presented the lowest values of WVP. This is suggested to happen due to an aggregation and self-condensation of pullulan and *β*-glucan particles at elevated concentrations, which can produce voids in the film matrix (Chang *et al*., 2019). The OP of the films was determined by a specific parameter named peroxide value (PV) of the oil. This principle states that lower peroxide values (grams of peroxide per 100g of film) allow better oxygen barrier of the membrane. According to Chang *et al*. (2019) the PV of the pullulan film was 1.193g/100g. Adding *β*-glucan decreased the PV value and therefore enhanced the OP of the blend films. The highest OP was observed in BP4 (pullulan-*β*-glucan = 0.15:0.15) film, with a PV value of 1.124g/100g. This indicates that *β*-glucan addition might improve OP (Chang *et al*., 2019). BP5 and BP6 films showed worse OP results and the pure *β*-glucan film presented the highest PV value when compared with the pure pullulan film. In conclusion, by blending high concentrations of *β*-glucan into the formulation, the film presents a structure similar to the *β*-glucan film but shows worse OP properties. In addition, the *β*-glucan addition to the film formulation enhanced several properties, including some mechanical properties (tensile strength, elongation), barrier properties (WVP, OP) and solubility. These findings are comparable to the previously mentioned study of arabinoxylan-*β*-glucan blend films since the results are quite similar. This might imply that *β*-glucan has an adequate compatibility with different film matrices and usually will enhance the functional properties of the composite films.

Some studies showed the ability to use *S. cerevisiae* in a dispersion form to formulate edible films. For this purpose, *S. cerevisiae* yeast is subjected to specific homogenization treatments at high pressure, followed by thermal treatment. Using yeast to replace traditional sources of biodegradable polymers can be a valuable option to generate sustainable edible films for the packaging industries. Investigation has been made to verify the benefits of using *β*-

glucans as a raw material to create edible films with adequate properties (Peltzer *et al*., 2018). Some suggested advantages and possible limitations/disadvantages by using *β*-glucan are described in Table 15.

Table 15 Advantages and disadvantages of *β*-glucans in the preparation of edible films.

Advantages	Disadvantages/Limitations
Essential properties for the edible film (gelling and permeability…)	Low solubility, depending on the *β*-glucan source.
Easy manipulation of properties (by changing glucan molecular ratio)	Low biocompatibility (when structural modification does not occur)
It is possible to introduce external substances to its structure (e.g. polyols)	High extraction and purification costs
Excellent applicability in several industries	Possible environmental impact by using the most common extraction methods

4.2 *S. cerevisiae* mannoproteins film forming properties

It is stated that mannose at high concentrations can act as a plasticizer if added to other films. Zhang & Han (2010) compared the properties of edible starch films with different plasticizers: glucose, fructose, sorbitol, glycerol, ethylene glycol and mannoproteins (specifically mannose). The mannose films presented low values of elongation at break compared to other conventional edible films. From 10 to 20% plasticizer concentration, their percentual elongation varied from 0.1 to 1%. The effect of crystallinity is also mentioned. At 8.7 to 19.3% crystallinity (10 to 15% of mannose respectively), the elongation at break of the film decreased to the lowest level among all tested films. Therefore, when crystallinity increases, elongation decreases. Mannose films also showed the highest elasticity modulus` when mannose had concentrations ranging from 10 to 20%. They also presented elastic characteristics rather than plastic; mannose provides mass transfer passage to oxygen, which in return increases the oxygen permeability ratio (Zhang & Han, 2010).

Abdolshahi et al. (2019) assessed the inhibition of *Aspergillus flavus* growth in pistachios by adding a coating onto the food product. The coating composition was based on mannoprotein extracts from the *S. cerevisiae* cell wall, incorporated in a gelatin-based solution. Several percentages of mannoprotein were tested, and the results are shown on the

Table 16.

Table 16 *Aspergillus flavus* growth in pistachio samples after incubation **[adapted from Abdolshahi *et al*., 2019].**

		Days								
Sample	**Mannoprotein (%)**	**1**	**2**	**3**	**4**	**5**	**6**	**7**	**8**	**9**
Non-coated	0.0	+ [a]	++ [b]	++	++	++	++	++	++	++
Coated	0.5	- [c]	-	-	-	-	+	+	+	++
	1.0	-	-	-	-	-	-	+	+	+
	1.5	-	-	-	-	-	-	-	-	+
Legend: [a] initial visible growth; [b] growth development; [c] no visible growth.										

Results showed that when pistachios were not coated, fungi appeared on the first 24 hours post-incubation. When a low-concentrated mannoprotein coating was applied, fungi only appeared on the sixth day post-incubation. By increasing the mannoprotein concentration, the antifungal effect became more efficient and stopped any growth development on the pistachio. Pistachios can then be protected against fungi for a period of at least one week. Within this study, mannoproteins were confirmed to have antifungal properties, which is an essential property to protect food products (Abdolshahi et al., 2019).

The effect of using a D-mannose-blend film was also assessed by Hou *et al*., (2013). The blends films were formed by silk fibroin and D-mannose, casted at different ratios. The first property analyzed was the water solubility. Figure 13 shows the different solubilities obtained for silk fibroin.

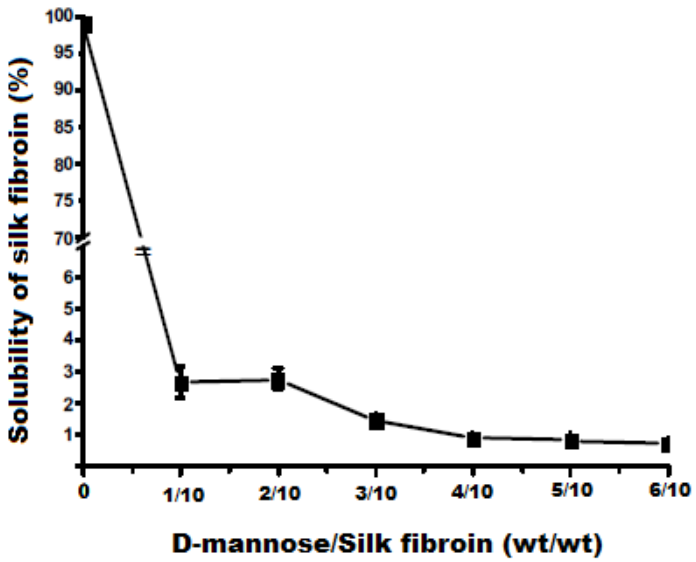

Figure 13 Solubility of blend films **[Hou *et al.*, 2013]**.

Figure 13 shows that pure silk fibroin had a dissolution rate of approximately 99%. Adding D-mannose onto the blend film (at a 10% weight ratio) immediately decreased solubility to 4%. Further addition of D-mannose made the blend film almost insoluble. Being a sugar, it possesses many hydroxyl groups that will crosslink with the hydrogen bonds of silk fibroin. In this specific case, silk fibroin also modified its structure which contributed to the dramatic decrease in solubility (Hou *et al.*, 2013). The strength and elongation of the blend films were also investigated. The same D-mannose ratios were used, and the results can be seen in the Figure 14.

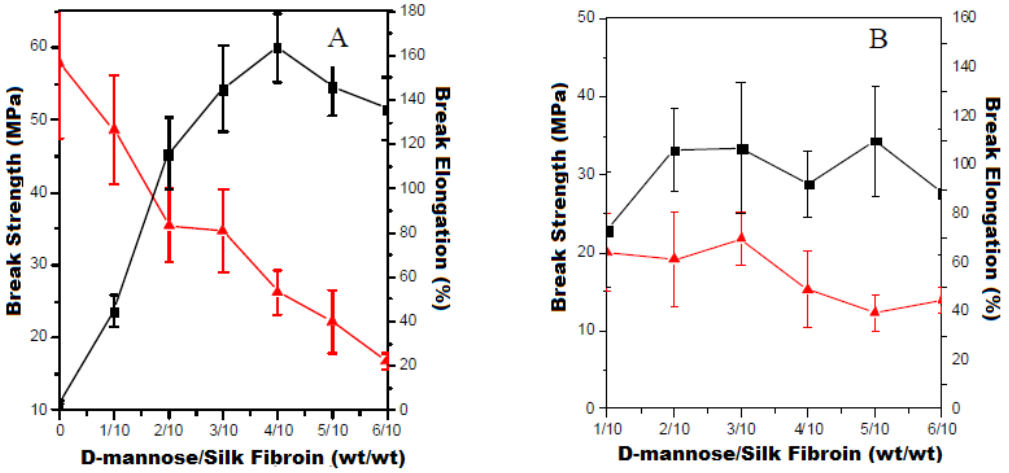

Figure 14 Strength and elongation of the blend films. A: dry state; B: wet state. ▲- Strength; ▪ - elongation **[Hou *et al.*, 2013]**.

By increasing the D-mannose content in the dry state (A) blend film, its tensile strength decreased, which might be explained by the plasticizer role played by the sugar. The blend film appears to have great flexibility, having an elongation of 160% at a ratio of 4/10 D-mannose/silk fibroin. Thus, it can be determined that adding small amounts of D-mannose will significantly increase the film's toughness. However, adding too much D-mannose will make the film more brittle (Hou *et al.*, 2013). In the wet state (B), D-mannose was eluted onto the film. This mechanism promoted a larger number of holes in the blended film. A higher mannose content increased the number of holes in the film and therefore its tensile strength and strain was reduced. Still, the blend films presented good flexibility, with an elongation at break of over 90% (Hou *et al.*, 2013). This film was intended to be applied on a corneal tissue, however, several conclusions can be transferred onto food packaging films. The main one is that mannose can allow a certain component to be practically insoluble, depending on the matrix used. Mannose is highly functional in terms of mechanical properties, highlighting the flexibility of a film. However, its tensile strength may be lowered.

Another component very similar to mannoproteins are galactomannans. Its properties may be very similar to mannoprotein-based films, so it is worth to investigate. Recent studies of galactomannans-based films showed promising properties. Dos Santos *et al*. (2015) studied five sources of galactomannans, *Adenanthera pavonina* (AP), *Cyamopsis tetragonolobus* (Guar gum = GG), *Caesalpinia pulcherrima* (CP), *Ceratonia siliqua* (Locust bean gum = LBG) and *Sophora japonica* (SJ). The mannose/galactose (M/G) ratios under study were 1.3, 1.7, 2.9, 3.4

and 5.6. Three gases were subjected to different analysis: water vapor permeability (WVP), oxygen (OP) and carbon dioxide (COP) permeabilities and solubility (%). The main results are shown in **Error! Reference source not found.**.

Table 17 Values of mannose/galactose ratio (M/G), water vapor (WVP), carbon dioxide (COP), oxygen permeabilities (OP) and solubility (%) for galactomannan-based films **[adapted from dos Santos *et al.*, 2015]**.

Galactomannan film	M/G	WVP × 10^{-11} g m^{-1} Pa^{-1} s^{-1}	COP × 10^{-15} g m $(Pa\ s\ m^2)^{-1}$	OP × 10^{-15} g m $(Pa\ s\ m^2)^{-1}$	Solubility (%)
AP	1.3	6.78 ± 0.63	28.81 ± 2.36	2.79 ± 0.14	64.39 ± 2.23
GG	1.7	10.45 ± 0.32	37.06 ± 0.93	1.85 ± 0.08	81.08 ± 7.78
CP	2.9	10.69 ± 0.75	42.90 ± 2.46	1.64 ± 0.08	92.75 ± 0.96
LBG	3.4	9.16 ± 0.70	37.16 ± 4.22	1.75 ± 0.31	26.80 ± 8.82
SJ	5.6	8.06 ± 0.29	28.74 ± 3.70	2.94 ± 0.08	44.35 ± 12.77

Legend: *Adenanthera pavonina* (AP), *Cyamopsis tetragonolobus* (Guar gum = GG), *Caesalpinia pulcherrima* (CP), *Ceratonia siliqua* (Locust bean gum = LBG) and *Sophora japonica* (SJ).

From Table 18, it is possible to understand that WVP and COP values increased for higher values of M/G ratio, up to a ratio of approximately 3. This is mainly due to a decrease in galactose content and a stronger influence of mannose onto the film, promoting a larger diffusion of water molecules. For M/G ratios higher than 3, WVP and COP behave in a different way. The SJ film with a ratio of 5. had low amounts of galactose, resulting in galactomannan chains with free mannan units. This promotes a dense packing of galactomannan chains, which disturbs the diffusion of water and carbon dioxide molecules. In conclusion, higher M/G ratios lead to an increase of free mannan units which increases intermolecular forces that will affect permeability. In terms of OP values, there is no clear conclusion as to why the intermediate M/G ratios present lower OP and the lower and highest M/G ratios present the largest OP values. It might be that the galactomannan source has an effect in the OP due to a different structural distribution of galactose (dos Santos *et al*, 2015).

The sensitivity of the films to water can be evaluated by measuring solubility and water content. Food applications may require water insolubility to enhance product integrity and water resistance, or good water solubility if the film is meant to be dissolved quickly (Pérez-

Gago & Krochta, 2001). This parameter was also evaluated by dos Santos et al, (2015). According to these authors, the solubility values increased continuously up to a M/G ratio of 3 (Table 17). For higher M/G values, solubility decreased significantly. The presence of a plasticizer like glycerol (a hydrophilic molecule) may reduce the hydrophobicity of galactomannan films. Also, its crystalline arrangement can influence their water solubility. For galactomannan films with higher M/G ratio, the hydrophobic mannan chains will contribute to decrease the water solubility of the films. This occurs due to a dense packing of mannan chains which generate stronger inter-chain bonds and consequently, more water-resistant films (dos Santos *et al*, 2015). The mechanical properties of the films were also assessed; results are displayed in Figure 15.

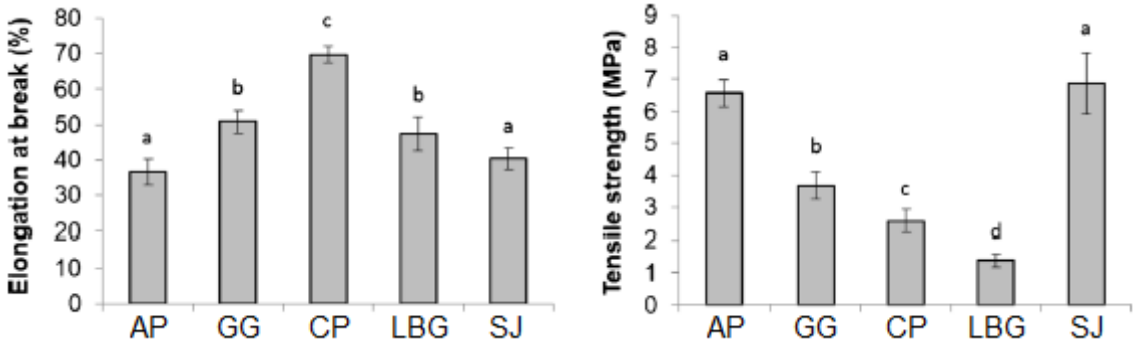

Figure 15 Elongation-at-break and tensile strength of AP, GG, CP, LBG and SJ galactomannan films **[dos Santos *et al*., 2015]**.

Legend: *Adenanthera pavonina* (AP), *Cyamopsis tetragonolobus* (Guar gum = GG), *Caesalpinia pulcherrima* (CP), *Ceratonia siliqua* (Locust bean gum = LBG) and *Sophora japonica* (SJ).

It is seen that elongation at break increases with the increase of the M/G ratio, up to the CP galactomannan films. For higher M/G ratios, elongation at break drops significantly. Tensile strength values follow an inverse behavior compared to elongation: they are high at low M/G ratios, rising again for high M/G ratios. A parallel study concluded that the depletion of galactose from the mannan chains makes the subsequent films to have higher elongation at break values. Another study stated that a high number of galactose units seems to obstruct galactomannan interactions with adjacent chains and this phenomenon seems to create more flexible films. Consequently, tensile strength values will tend to decrease while the elongation

increases. The high tensile strength value on the SJ galactomannan film is explained by the dense packing of mannan chains (dos Santos *et al*, 2015).

The study of D-mannose application in polymeric films such as the *β*-glucan-protein based films is still on an initial and primitive stage. The fact that D-mannose has an inherent biological origin also limits its structural modification (Hussam *et* al., 2016). Therefore, it is concluded that while D-mannose presents many benefits, it also shows some drawbacks. **Error! Reference source not found.** summarizes some proposed advantages and disadvantages of using mannose in a film.

Table 18 Advantages and disadvantages of mannose in the preparation of edible films.

Advantages	Disadvantages/Limitations
High water solubility	Non-soluble in some reagents (e.g., ethanol)
Low caloric value	Limited structural modification due to its biological nature
Odorless	Limited industrial use and development
Stable at room temperature	
High biocompatibility	Primitive studies of the molecule
Diverse potential of application	

4.3 *S. cerevisiae β*-glucans-mannoproteins film forming properties

Generally, edible films based on polysaccharides present better WVP properties while films based on proteins show better mechanical properties. Therefore, by using both polysaccharides and proteins into formulating an edible film, it is possible to combine the best properties of two distinct edible film groups (Peltzer *et al.*, 2018). Until date, there is no research found that combines both *β*-glucans and mannoproteins into a film formulation. Therefore, it can be only be considered isolated cases of *β*-glucan films and mannoprotein films and expect that its synthesis will also combine properties from both groups. Alternative studies of protein-polysaccharide edible films can be highlighted to compare and understand the potential properties of the *β*-glucan-mannoprotein edible film.

Yoo *et al*. (2011) prepared isolated whey protein (WPI)-based films blended to different polysaccharides: regular starch (RS), amylopectin-based starch (APS), methylcellulose (MC), hydroxypropylmethylcellulose (HPMC) and sodium alginate (SA). The highest oxygen permeability (OP) was verified in MC and HPMC, and both are the less polar molecules of all

the polysaccharides tested. HPMC and MC are molecules with a great degree of substitution of hydroxyl groups. The less hydroxyl groups, the less polar the molecule becomes. Thus, the HPMC-WPI and MC-WPI film present a greater OP when compared to SA-WPI, RS-WPI or APS blended films (Yoo *et al.*, 2011).

These authors also tested the tensile strength of films. Each polymer chain of MC and HPMC consists of modified D-glucose units linked by β-(1 → 4)-glycosidic bonds which are more stable. Moreover, significant numbers of hydroxyl groups exist and allow the formation of hydrogen bonds between parallel polymer chains, resulting in high tensile strength in films made of MC or HPMC (Yoo *et al.*, 2011). The film's elongation at break was also evaluated. Adding different ratios of polysaccharides improved the percentual elongation. The RS-WPI and APS-WPI presented a notoriously higher percentual elongation when compared with the other film matrices. This might occur due to the superior sensitivity of starch when the plasticizer is added onto the film (Yoo *et al.*, 2011). Another remark can be made when observing the ratio of polysaccharides in the film: between 25 to 75% of starch added, the elongation has optimal values. This reinforces the idea that preparing a blend film with similar ratios of two components usually presents ideal properties, probably due to the symbiotic interactions that can occur in proteins and polysaccharides.

More recently, Chakravartula *et al*. (2019) prepared edible films based on a whey protein matrix combined with two different polysaccharides (pectin and alginate). Both polysaccharides are often used in edible film formulations. Pectin films are characterized by high WVP, which in return may act to prevent dehydration of food products. Alginates can form synergistic gels when combined with pectin, under appropriate pH conditions. Thus, they are crucial to form an adequate edible film with improved mechanical properties. Whey protein possess great mechanical and barrier properties and whey protein films are highly regarded by their transparency, flexibility and good water, gas, aroma, and oil barrier characteristics. Furthermore, a suitable thermal degradation denatures whey proteins, which can result in more cohesive and stronger films when compared to its native state (Chakravartula *et al.*, 2019). These authors evaluated the pH of the film-forming solutions to understand its ionic nature, since it can affect the stability and functionality of the solutions. The viscosity parameter (μ) was also assessed, due to its high influence on absorption and adhesion to the matrix, as well as on the film thickness, uniformity, and microstructure (Chakravartula *et al.*, 2019). The main results are shown in Table 19.

Table 19 Physical and mechanical properties of the edible films **[Adapted from Chakravartula et al., 2019]**.

Sample %w/w (P/A/WP)	pH	M (mPa s)	Thickness (µm)	Yellowness index	Opacity	E (MPa)	σ^B (MPa)	ε^B (%)
S_1 (1:1:1)	4.80 ± 0.01	247.0 ± 1.27	45 ± 4	9.3 ± 0.9	6.0 ± 0.2	444 ± 107	23 ± 6	22 ± 9
S_2 (3:0:0)	3.43 ± 0.01	272.0 ± 7.00	36 ± 1	9.6 ± 1.1	3.4 ± 0.1	1467 ± 303	62 ± 20	20 ± 8
S_3 (1.5:1.5:0)	4.12 ± 0.01	249.0 ± 1.53	43 ± 2	7.5 ± 0.4	2.9 ± 0.1	958 ± 240	61 ± 11	23 ± 10
S_4 (0:1.5:1.5)	6.29 ± 0.03	46.2 ± 2.26	47 ± 1	11.6 ± 0.5	5.0 ± 0.2	406 ± 145	22 ± 9	40 ± 23
S_5 (1.5:0:1.5)	4.48 ± 0.04	*	64 ± 2	12.5 ± 0.9	3.0 ± 0.1	352 ± 140	13 ± 4	16 ± 7
S_7 (2:0.5:0.5)	6.22 ± 0.06	*	43 ± 2	9.2 ± 1.3	5.3 ± 0.2	555 ± 129	27 ± 5	26 ± 4
S_8 (0.5:2:0.5)	4.14 ± 0.03	154.0 ± 7.83	41 ± 1	8.5 ± 0.5	4.1 ± 0.3	746 ± 127	31 ± 10	24 ± 12
S_9 (0.5:0.5:2)	4.98 ± 0.1	143.0 ± 2.47	49 ± 1	10.7 ± 0.4	5.2 ± 0.2	288 ± 59	11 ± 3	19 ± 2
S_{10} (0:3:0)	5.50 ± 0.01	45.1 ± 0.88	42 ± 1	4.3 ± 0.1	3.7 ± 0.4	607 ± 243	39 ± 16	27 ± 14

Legend: (µ) viscosity; **(E)** elastic modulus; **(σ^B)** tensile strength at break; **(ε^B)** elongation at break.

Results from Table 19 showed that the pH value is directly influenced by the components in the solution, with alginate and whey protein increasing its value. Pectin decreased the pH to acidic values, which is expected since commercial pectin forms solutions have pH 3.0-4.0. All the film forming solutions presented viscosity values ranging from 120 to 250 mPa s, except samples S_4, S_6 and S_9 in which whey protein content was higher than 1% w/w, presenting values lower than 50 mPa s. Authors suggested that the presence of whey protein tends to decrease the viscous nature of pectin and alginate, which may be attributed to strong associative interactions between the polysaccharide and protein components (Chakravartula *et al*., 2019). The mechanical properties of the films were also assessed. Parameters such as thickness, yellowness index, opacity, elastic modulus (E), tensile strength at break (σ^B) and elongation at break (ε^B) were studied (Chakravartula *et al*., 2019). Sample 6 was excluded from the tests because due to its low concentration on whey protein, it did not fulfill some requirements needed to determine some of the properties mentioned. The thickness of the films varied from 36 to 64 μm. This variance was somewhat expected, which can be attributed to the slight difference in film drying kinetics and interactions that occur in the composite matrix of the films. The optical properties, such as opacity and yellowness, are a crucial aspect for edible films to be accepted by customers. Generally, they are expected to be colorless or at least close to the food color onto which the edible film will be applied. The alginate films were more visually transparent, followed by pectin and whey protein films. This negative effect in transparency can be attributed to the formation of insoluble protein-polysaccharide aggregates during drying or due to the presence of immiscible dispersed phases in the final composite film. The yellowness index was calculated to estimate the perceived yellowness, as low yellow value is generally preferred. It was concluded that higher concentration of pectin and whey protein increased the yellowness index (Chakravartula *et al*., 2019). The tensile strength values varied from 11 to 62 MPa, with the lowest values found in S_5 (1.5:0:1.5) and S_9 (0.5:0.5:2) samples. Pectin, alginate and the interaction of pectin/whey protein were observed to be primary factors affecting the tensile strength of the films, with pectin and alginate increasing, and pectin/whey protein decreasing the tensile strength value. Interactions between alginate/whey protein were non-significant. This behavior was similarly found in the elastic modulus, with pectin and alginate increasing the final value, whereas whey protein interactions with pectin and alginate decreased it (Chakravartula *et al*., 2019). The barrier properties of the films, as well as their moisture content were determined. The results are shown in Table 20.

Table 20 Moisture content, water vapor, oxygen and carbon dioxide permeabilities of the edible films **[Adapted from Chakravartula *et al*., 2019]**.

Sample %w/w (P/A/WP)	Moisture content (%)	WVP (10^{10} g mm h^{-1} cm^{-1} Pa^{-1})	OP (cm^3 $m^{-2}d^{-1}$ bar^{-1})	COP (cm^3 $m^{-2}d^{-1}$ bar^{-1})
S_1 (1:1:1)	12.2 ± 1.7	7.9 ± 0.4	16 ± 21	68 ± 2
S_2 (3:0:0)	8.6 ± 1.1	7.3 ± 0.4	10 ± 2	119 ± 2
S_3 (1.5:1.5:0)	6.6 ± 1.3	7.4 ± 0.3	49 ± 3	123 ± 2
S_4 (0:1.5:1.5)	13.7 ± 1.4	8.7 ± 1.1	83 ± 1	87 ± 2
S_5 (1.5:0:1.5)	11.9 ± 0.6	9.6 ± 0.5	1023 ± 3	115 ± 4
S_7 (2:0.5:0.5)	6.8 ± 1.1	7.9 ± 0.2	166 ± 1	303 ± 6
S_8 (0.5:2:0.5)	7.4 ± 0.5	7.5 ± 0.4	17 ± 3	75 ± 4
S_9 (0.5:0.5:2)	10.8 ± 1.3	9.0 ± 0.1	149 ± 4	152 ± 4
S_{10} (0:3:0)	8.5 ± 1.6	7.2 ± 0.1	438 ± 16	1043 ± 59

The moisture content was measured to estimate the water bonding capacity of the films. The values varied from 6.6 to 13.7%, in some cases with higher numbers due to significant influence of WP concentration and linear interactions (such as P/A, P/WP or A/WP). The hygroscopic nature of glycerol (plasticizer) also favored the absorption of water molecules and the formation of hydrogen bonds in the matrix, leading to a higher moisture content (Chakravartula *et al*., 2019). The WVP ranged from 7.2 to 9.6 (10^{10} g mm h^{-1} cm^{-1} Pa^{-1}). Pectin-based and alginate-based films presented the lowest values, whereas whey protein slightly increased the permeability values. This might be attributed to a higher number of free hydroxyl groups, which in return enhances interaction with water and favors water vapor transmission (Chakravartula *et al*., 2019). The gas transmission rate is found to be affected by the composition of the films. In this case, the highest gas permeation (composed by an average of OP and COP) was attributed to the pure alginate film. The pure pectin film showed a lower permeability when compared to alginate. In general, adding WP to the matrix decreased the permeability. Gas permeability through matrices is complex because there are several parameters that affect it. Some relate to the gas characteristics such as molecular size, polarity, or activity; others are linked to material properties, such as degree of crystallinity, presence of cross-linking, or chain stiffness. The general idea is that a more tortuous gas path leads to a lower gas transmission rate. Usually CO_2 permeation, when compared to O_2 permeation, shows very different values in the same sample, often being lower. This phenomenon was not clear in

the samples analyzed due to the higher affinity (high solubility) of CO_2 gas molecules within this type of matrix (Chakravartula *et al*., 2019).

Other studies show different composite edible films used mostly into food formulations. These are represented in Table 21, as well as the main conclusions and benefits withdrawn from the investigation.

Table 21 Improved properties of composite protein-polysaccharide edible films.

Edible film	Observations	References
Chitosan + gelatin	Microbial decomposition decreased in peppers; improved peppers texture and extended the cold storage and shelf-life period, without affecting the nutritional value.	Poverenov *et al*. (2014)
Starch + gelatin	Coated grapes had improved appearance after storage under refrigerated conditions; lower weight loss compared with the control group.	Fakhouri *et al*. (2015)
Starch + pea protein	Increased tensile strength; prevented humidity-induced shrinkage; improved blown-film processability and barrier properties.	Huntrakul *et al*. (2020)
Starch + carrageenan gum	Higher melting point; lower water vapor permeability; lower solubility; higher transparency.	Sandhu *et al*. (2019)
Alginate + soy protein	Increased the percentage of elongation at break; Higher gelling property and water resistance; Uniform surface structure.	Pan *et al*. (2014)

Several patents of *β*-glucan are found in the market, such as a cold water soluble *β*-glucan product that can be used into edible films (Morgan, 2004) and *β*-glucans from cereals like oat that are used in edible films or coatings (Redmond, 2001). In case of mannoprotein-based films, there is no patent found that applies this material to food packaging products. The same conclusion was found for the *β*-glucan-mannoprotein-based edible films.

5 Concluding remarks

A summary of the main findings and suggestions for future research are presented in sections 5.1 and 5.2, respectively.

5.1 Summary of the main conclusions

This thesis focused on the study of edible films with *β*-glucans and mannoproteins.

Chapter 1 introduced the generational trends of biopolymers, in which it was possible to understand that the current criteria for biopolymers is based on its biodegradability and sustainability. A succinct market analysis of biopolymers used for packaging was made, stating that its market value is around €533 billion, and substituting conventional packaging for sustainable packaging would be economically and environmentally impactful. A general view on the EU strategies to combat plastic challenges was also mentioned and distinct concepts of "biofilm", "edible film" and "coating" were explained.

In Chapter 2, the main film forming properties were thoroughly studied. Regarding the antimicrobial activity it was concluded that several groups of polysaccharides and proteins – including the *β*-glucans and mannoproteins, - can be used as antimicrobial agents to control pathogenic populations and improve the food product's shelf life. The amino acid groups play an important role in the antioxidant mechanisms, since mannoproteins and *β*-glucans contain those amino acids, their based edible films could present high antioxidant activity. Also, the anti-inflammatory action was explained, concluding that *β*-glucans and mannoproteins possess an anti-inflammatory response. The mechanical properties of polymers, as well as their classification based on their behavior when various tensile stresses are applied was also mentioned. The concept of permeability was clarified, as well as the classification of water permeability and oxygen permeability, followed respectively by their standard mass transfer equations and kinetic models. Finally, the thermal properties were explained, as well as typical thermal analysis techniques such as DSC and TGA; and the mathematic deductions of enthalpic equations and the most common kinetics of the reaction models were explained.

Chapter 3 described in detail the cell wall structure of *Saccharomyces cerevisiae*, showing that the major components in the cell wall are *β*-glucans (55-65% dw) and mannoproteins (35-40% dw). Deeper structural description of mannoproteins and *β*-glucans was made, as well as some of their most recognized biological properties. The methods for

isolation and characterization of β-glucans and mannoproteins were described, being concluded that the most used extraction methods are heat treatment, alkaline extraction, SDS extraction and enzymatic treatment. All these methods require several stages of centrifugation; chromatography techniques are also used, being more suitable for laboratory scale extractions.

In Chapter 4, the β-glucan-based film forming properties were characterized, being possible to state that films are water insoluble, compact, non-porous, non-crystalline and have improved properties when a plasticizer like glycerol is used in concentrations up to 25%. The same analysis was made for mannoprotein-based films, these films present good elastic properties, as well as water vapor and oxygen permeabilities, but an increment in crystallinity leads to a decrease in elongation. The literature does not present any information regarding the combination of mannoproteins and β-glucans in an edible film. That was the primary focus on this research work. However, due to the COVID-19 pandemic, laboratories were shut down and it was decided that it would only be possible to study the literature available and compile the information regarding these films; this would eventually mean that the dissertation would become a monography.

Based on the current assigned patents, β-glucan edible films are being used in the industry. The same cannot be said of mannoprotein and mannoprotein-β-glucan edible films since there is no patent associated with its development or manufacture.

5.2 Directions for future research

This dissertation revealed that there is a huge potential in edible films made from biodegradable and renewable sources. While films are quite well developed in laboratory, an emergent need for an up-scale of the manufacturing process is required. This way, it would be possible to not only develop environmentally friendly solutions for the packaging industry but also to accomplish the European Strategy for Plastics in a Circular Economy, which states that all plastics packaging in the EU must be reusable or recyclable in a cost-effective manner by 2030.

Yeast-based films were already developed in the past. Still, there is no current investigation regarding edible films based on the combination of β-glucans and mannoproteins,

which in theory would have improved mechanical, rheological, and textural properties, as well as improved antioxidant and antimicrobial action against oxidative reactions and pathogens, respectively. In these films, permeation of water vapor and oxygen appears to be well controlled and optimal, increasing shelf-life of food products. While some research about β-glucan films exist, the research level of mannoprotein films is almost inexistent. Therefore, further investigation and development of these edible films is encouraged.

Usually the plasticizer of choice is glycerol, but there is a broad range of plasticizers to select, such as Polyethylene glycol of low molecular weight (PEG 400), which was the plasticizer initially intended to test along with glycerol. Thus, it is recommended to test several plasticizers of different origins, to find the one that suits the best in the edible film. Furthermore, it is noticed that the extraction methods for β-glucans and mannoproteins are still in a primitive state of optimization. Thus, it might be necessary to adopt new methods to obtain higher extraction yields. Although some of the methods that are currently used do not contain associated hazardous substances, they use high quantities of reagents. Thus, the application of green methods is advised to avoid excessive reagent effluents.

References

Abdolshahi, A., Marvdashti, L., Salehi, B., Sharifi-Rad, M., Ghobakloo, S., Iriti, M. (2019). *Antifungal activities of coating incorporated with Saccharomyces cerevisiae cell wall mannoprotein on Aspergillus flavus growth and aflatoxin production in pistachio (Pistacia vera L.)*. Journal of Food Safety 39(2).

Abdolshahi, A., Yazdi, F.T., Shabani, A., Mortazavi, S.A., Nafchi, A.M. (2016). "*Antifungal properties of gelatin-based coating containing mannoprotein from saccharomyces cerevisiae on aspergillus flavus growth in pistachio"*. Journal of Mazandaran University of Medical Sciences 26(139), 93-102.

Action International. "*Beta 1,3/1,6 Glucan*". https://www.action-inter.net/beta-1316-glucan.html – accessed on November 11, 2019.

Azeredo, J., Azevedo, N. F., Briandet, R., Cerca, N., Coenye, T., Costa, A. R., Jaglic, Z. (2017). *Critical review on biofilm methods*. Critical Reviews in Microbiology 43(3), 313-351.

Bastos, R., Coelho, E., & Coimbra, M. A. (2015). *Modifications of Saccharomyces pastorianus cell wall polysaccharides with brewing process*. Carbohydrate Polymers 124, 322-330.

Blahovec, J., Hejlová, A., Čopíková, J., Novák, M. (2011). *Tensile properties of microbial β-glucan films*. Polymer Engineering & Science 51(12), 2564-2570.

Blasco, L., Viñas, M., & Villa, T. (2011). *Proteins influencing foam formation in wine and beer: the role of yeast*. International Microbiology 14(2), 61-71.

Bourtoom, T., Chinnan, M. S., Jantawat, P., Sanguandeekul, R. (2006). *Effect of Plasticizer Type and Concentration on the Properties of Edible Film from Water-Soluble Fish Proteins in Surimi Wash-Water*. Food Science & Technology International 12(2), 119-126.

Brindzová, L., Čertík, M., Rapta, M., Zalibera, M., Mikulajová, A., Takácsová, M. (2008). *Antioxidant Activity, β-Glucan and Lipid Contents of Oat Varieties*. Czech Journal of Food Science 26(3), 163-173.

Cao, Y., Sun, Y., Zou, S., Duan, B., Sun, M., Xu, X. (2018). *Yeast β-glucan Suppresses the Chronic Inflammation and Improves the Microenvironment in Adipose Tissues of ob/ob Mice*. Journal of Agricultural and Food Chemistry 66(3), 621-629.

Chakravartula, S. S. N., Soccio, M., Lotti, N., Balestra, F., Rosa, M. D., Siracusa, V. (2019). *Characterization of Composite Edible Films Based on Pectin/Alginate/Whey Protein Concentrate*. Materials 12(15), 2454.

Chang, J., Li, W., Liu, Q., Zhou, Y., Chen, X., Lyu, Q., Liu, G. (2019). *Preparation, properties, and structural characterization of β-glucan/pullulan blend films*. International Journal of Biological Macromolecules 140, 1269-1276.

Chen, J. & Seviour, R. (2007). *Medicinal importance of fungal beta-(1-->3), (1-->6)-glucans*. Mycological Research 111(6), 635-52.

Chen, Y., Dong, L., Liu, F., Song, L., Li, C., Tang, W., Chen, J. (2013). *1,3-β-Glucan affects the balance of Th1/Th2 cytokines by promoting secretion of anti-inflammatory cytokines in vitro*. Molecular Medicine Reports 8, 708-712.

Colby College. *Differential Scanning Calorimetry; First and Second Order Transitions in Polymers*. https://www.colby.edu/chemistry/PChem/lab/DiffScanningCal.pdf - (accessed on April 11, 2020)

Delgado, J. F., Peltzer, M. A., Wagner, J. R., & Salvay, A. G. (2018). *Hydration and water vapour transport properties in yeast biomass based films: A study of plasticizer content and thickness effects*. European Polymer Journal 99, 9-17.

Delgado, J. F., Sceni, P., Peltzer, M. A., Salvay, A. G., de la Osa, O., Wagner, J. R (2016). *Development of innovative biodegradable films based on biomass of Saccharomyces cerevisiae*. Innovative Food Science & Emerging Technologies 36, 83-91.

Dikit, P., Maneerat, S., Musikasang, H., H-kittikun, A. (2010). "*Emulsifier properties of the mannoprotein extract from yeast isolated from sugar palm wine*". ScienceAsia 36(3), 312-318.

dos Santos, V.R.F., Souza, B.W.S., Teixeira, J.A., Vicente, A.A., Cerqueira, M.A. (2015). *Relationship between galactomannan structure and physicochemical properties of films produced thereof*. Journal of Food Science and Technology 52, 8292-8299.

Endres, H. J., & Siebert-Raths, A., 2011. *Engineering Biopolymers: Markets, Manufacturing, Properties and Applications*. 1st Edition. Hanser Publishers. 691pp.

Fakhouri, M. F., Martelli, S. M., Caon, T., Velasco, J. I., Mei, L. H. I. (2015). *Edible films and coatings based on starch/gelatin: Film properties and effect of coatings on quality of refrigerated Red Crimson grapes*. Postharvest Biology and Technology 109, 57-64.

Falguera, V., Quintero, J. P., Jiménez, A., Muñoz, J. A., Ibarz, A. (2011). *Edible films and coatings: Structures, active functions and trends in their use*. Trends in Food Science & Technology 22(6), 292-303.

Feedipedia. "*Brewers yeast*". December 13, 2018. https://www.feedipedia.org/node/72 (accessed on April 25, 2020)

Fiocchi, C. (2008). "*What is "physiological" intestinal inflammation and how does it differ from "pathological" inflammation?*". Inflammatory Bowel Diseases 14(2), 77-78.

Graham, D., 2003. "*Power supplies. Use of Electricity in Food Technology*". Encyclopedia of Food Sciences and Nutrition. 2nd Edition. Elsevier. 6000pp.

Han, J. H., 2005. "*Innovations in Food Packaging*". Food Science and Technology International. 1st Edition. Academic Press. 509pp.

Hatakeyama, T., & Quinn, F., 1999. *Thermal analysis: fundamentals and applications to polymer science*. 2nd Edition. Wiley. 190pp.

Hou, J., Qian, Q., Zhang, S., Shen, Y., Lu, S. (2013). *Study on Silk Fibroin D-mannose Blend Films*. Advanced Materials Research 796, 112-116.

Huntrakul, K., Yoksan, R., Sane, A., Harnkarnsujarit, N. (2020). Effects of pea protein on properties of cassava starch edible films produced by blown-film extrusion for oil packaging. Food Packaging and Shelf Life 24, 100480.

IPI Singapore. “High Value Added Completely Biodegradable Packaging Materials from Agricultural Residues.” September 2, 2019. https://www.ipi-singapore.org/technology-offers/high-value-added-completely-biodegradable-packaging-materials-agricultural. (Accessed in June 10, 2020)

Jaehrig, S. C., Rohn, S., Kroh, L. W., Fleischer, L., Kurz, T. (2007). *In Vitro Potential Antioxidant Activity of (1→3),(1→6)-β-D-Glucan and Protein Fractions from Saccharomyces cerevisiae Cell Walls*. Journal of Agricultural and Food Chemistry 55, 4710-4716.

Jawaid, M., Thariq, M., & Saba, N. (2018). *Mechanical and Physical Testing of Biocomposites, Fibre-Reinforced Composites and Hybrid Composites*. 1st Edition. Woodhead Publishing. 478pp.

Johnson, C., Hashim, M., Bailey, C., Byrd, J., Kogut, M., Arsenault, R. (2020). *Feeding of yeast cell wall extracts during a necrotic enteritis challenge enhances cell growth, survival and immune signaling in the jejunum of broiler chickens*. Poultry Science 99(6), 2955-2966.

Jongjareonrak, A., Benjakul, S., Visessanguan, W., Tanaka, M. (2006). *Effects of plasticizers on the properties of edible films from skin gelatin of bigeye snapper and brownstripe red snapper*. European Food Research and Technology 222(3), 229-235.

Kaliappan, S. K. (2007). *Characterization of physical properties of polymers using AFM force-distance curves*. Doctoral thesis in Science, Department of Chemical Biology of Siegen University. 113pp.

Kaur, R., Sharma, M., Ji, D., Xu, M., & Agyei, D. (2020). *Structural Features, Modification, and Functionalities of Beta-Glucan*. Fibers 8(1), 1.

Kirin Holdings. “*Kirin Beer University Report Global Beer Production by Country in 2018*”. October 3, 2019. https://www.kirinholdings.co.jp/english/news/2019/1003_01.html (accessed on April 25, 2020)

Klis, F. M., Mol, P., Hellingwerf, K., & Brul, S. (2002). *Dynamics of cell wall structure in Saccharomyces cerevisiae*. FEMS Microbiological Review 26(3), 239-256.

Kofuji, K., Aoki, A., Tsubaki, K., Konishi, M., Isobe, T., Murata, Y. (2012). *Antioxidant Activity of β-Glucan*. ISRN Pharmaceutics, 125864.

Kristinsson, H. G., Hultin, H. O. (2003). *Effect of low and high pH treatment on the functional properties of cod muscle proteins*. Journal of Agricultural and Food Chemistry 51(17), 5103-5110.

Kuorwel, K. K., Cran, M. J., Sonneveld, K., Miltz, J., & Bigger, S. W. (2011). *Antimicrobial activity of biodegradable polysaccharide and protein-based films containing active agents*. J Food Sci, 76(3), 90-102.

Li, J., Karboune, S., & Asehraou, A. (2020). *Mannoproteins from inactivated whole cells of baker's and brewer's yeasts as functional food ingredients: Isolation and optimization*. Journal of Food Science 85(5), 1438-1449.

Luo, J., Cheng, L., Du, Y., Mao, X., He, J., Yu, B., Chen, D. (2020). *The anti-inflammatory effects of low- and high-molecular-weight beta-glucans from Agrobacterium sp. ZX09 in LPS-induced weaned piglets*. Food & Function 11(1), 585-595.

Martínez, J. M., Cebrián, G., Álvarez, I., & Raso, J. (2016). *Release of mannoproteins during Saccharomyces cerevisiae autolysis induced by pulsed electric field*. Frontiers in Microbiology 7, 1435.

Methacanon, P., Weerawatsophon, U., Tanjak, P., Rachtawee, P., Prathumpai, W. (2011). *Interleukin8 stimulating activity of low molecular weight β-glucan depolymerized by γ-irradiation*. Carbohydrate Polymers 86(2), 574-580.

Mettler Toledo. "Thermal Analysis of Biopolymers". https://www.mt.com/us/en/home/library/on-demand-webinars/lab-analytical-instruments/Biopolymers_TA.html. (accessed on April 2, 2020).

Morgan, K. (2004). *Cold water soluble beta-glucan product and process for preparing the same*. U.S. Patent Application No. 10/312,969.

Muramatsu, M., Okura, M., Kuboyama, K., Ougizawa, T., Yamamoto, T., Nishihara, Y., Saito, Y., Ito, K., Hirata, K., Kobayashi, K. (2003). *Oxygen permeability and free volume hole size in ethylene–vinyl alcohol copolymer film: temperature and humidity dependence*. Radiation Physics and Chemistry 68(3-4), 561-564.

Netzsch Thermal Analysis. “Glass Transition Temperature”. https://www.netzsch-thermal-analysis.com/en/contract-testing/glossary/glass-transition-temperature/- (accessed on April 2, 2020).

Netzsch Thermal Analysis. “Crystallization Temperatures and Enthalpies”. https://www.netzsch-thermal-analysis.com/en/contract-testing/glossary/crystallization-temperatures-and-enthalpies/ - (accessed on April 2, 2020).

Ng, H., Saidi, N. M., Omar, F. S., Ramesh, K., Ramesh, S., Bashir, S. (2002). *Thermogravimetric Analysis of Polymers*. Encyclopedia of Polymer Science and Technology 1-29.

Nimse, S. B. & Pal, D. (2015). “*Free radicals, natural antioxidants, and their reaction mechanisms*”. RSC Advances 5, 27986-28006.

Novák, M., Synytsya, A., Gedeon, O., Slepička, P., Procházka, V., Synytsya, A., Blahovec, J., Hejlová, A., Čopíková, J. (2012). *Yeast β (1-3), (1-6)-d-glucan films: preparation and characterization of some structural and physical properties*. Carbohydrate Polymers 87(4), 2496-2504.

Padgett, T., Han, I., & Dawson, P. J. (1998). *Incorporation of food-grade antimicrobial compounds into biodegradable packaging films*. Journal of Food Protection, 61(10), 1330-1335.

Padgett, T., Han, Y., Dawson, P. (2000). *Effect of lauric acid addition on the antimicrobial efficacy and water permeability of corn zein films containing nisin*. Journal of Food Processing and Preservation 24(5), 423-432.

Pan, H., Jiang, B., Chen, J., Jin, Z. (2014). *Blend-modification of soy protein/lauric acid edible films using polysaccharides*. Food Chemistry 151, 1-6.

Peltzer, M., Delgado, J. F., Salvay, A. G., & Wagner, J. R. (2018). *β-Glucan, a promising polysaccharide for bio-based films developments for food contact materials and medical applications*. Current Organic Chemistry 22(12), 1249-1254.

Peltzer, M. A., Salvay, A., Delgado, J. F., de la Osa, O., Wagner, J. R. (2018). *Use of residual yeast cell wall for new biobased materials production: Effect of plasticization on film properties*. Food and Bioprocess Technology 11(11), 1995-2007.

Perez-Gago, M. B., & Krochta, J. M. (2001). *Denaturation time and temperature effects on solubility, tensile properties, and oxygen permeability of whey protein edible films*. Journal of Food Science, 66(5), 705-710.

Pintado, C. M., Ferreira, M. A., & Sousa, I. (2010). *Control of pathogenic and spoilage microorganisms from cheese surface by whey protein films containing malic acid, nisin and natamycin*. Food Control 21(3), 240-246.

Pokorný, J., Yanishlieva, N., & Gordon, M., 2001, *Antioxidants in food: practical applications*. 1st Edition. Elsevier. 400pp.

Polymer Database. "Stress-Strain Behavior of Polymers". https://polymerdatabase.com/polymer%20physics/Stress-Strain%20Behavior.html - (accessed on April 15, 2020)

Posadas, J. S., Caz, V., Caballero, I., Cendejas, E., Quilez, I., Largo, C., Elvira, M., de Miguel, E. (2010). *Effects of Mannoprotein E1 in Liquid Diet on Inflammatory Response and TLR5 Expression in the Gut of Rats Infected by Salmonella Typhimurium*. BMC Gastroenterology 10, 58.

Poverenov, E., Zaitsev, Y., Arnon, H., Granit, R., Alkalai-Tuvia, S., Perzelan, Y., Weinberg, T., Fallik, E. (2014). *Effects of a composite chitosan–gelatin edible coating on postharvest quality and storability of red bell peppers*. Postharvest Biology and Technology 96, 106-109.

Redmond, M. J. (2001). *Cereal beta glucan compositions and methods of Formulation*. U.S. Patent No 6,284,886.

Salgado, P. R., Ortiz, C. M., Musso, Y. S., Di Giorgio, L., & Mauri, A. N. (2015). *Edible films and coatings containing bioactives*. Current Opinion in Food Science 5, 86-92.

Sandhu, K. S., Sharma, K., Kaur, M., Kaur, R. (2019). *Physical, structural and thermal properties of composite edible films prepared from pearl millet starch and carrageenan gum:*

Process optimization using Response Surface Methodology. International Journal of Biological Macromolecules 143, 704-713.

Sárossy, Z., Tenkanen, M., Pitkänen, L., Bjerre, A., Plackett, D. (2012). *Extraction and chemical characterization of rye arabinoxylan and the effect of b-glucan on the mechanical and barrier properties of cast arabinoxylan films*. Food Hydrocolloids 30, 206-216.

Silva, P. (2017). Slides available on Moodle. Subject: Materials and Applications. Instituto Superior de Engenharia do Porto. - (accessed on April 15, 2020)

Shokri, H., Asadi, F., & Khosravi, A. R. (2008). *Isolation of β-glucan from the cell wall of Saccharomyces cerevisiae*. Natural Product Research 22(5), 414-421.

Stewart, G. G., Russell, I., & Anstruther, A., 2017, *Handbook of brewing*. 3rd Edition. CRC Press.

Supapvanich, S., Prathaan, P., Tepsorn, R. (2012). *Browning inhibition in fresh-cut rose apple fruit cv. Taaptimjaan using konjac glucomannan coating incorporated with pineapple fruit extract*. Postharvest Biology and Technology 73, 1-4.

Suchecka, D., Harasym, J., Wilczak, J., Gajewska, M., Oczkowski, M., Gudej, S., Błaszczyk, K., Kamola, D., Filip, R., Gromadzka-Ostrowska, J. (2015). *Antioxidative and anti-inflammatory effects of high beta-glucan concentration purified aqueous extract from oat in experimental model of LPS-induced chronic enteritis*. Journal of Functional Foods 14, 244-254.

Tejinder, S., Bhupinder, K., Harinder, K. (2000) *Flow behavior and functional properties of barley and oat water-soluble β-D-glucan rich extractions*, International Journal of Food Properties, 3(2), 259-274.

Temelli, F. (1997). *Extraction and functional properties of barley β-glucan as affected by temperature and pH*. Journal of Food Science 62(6), 1194-1201.

Thammakiti, S., Suphantharika, M., Phaesuwan, T., Verduyn, C. (2004). *Preparation of spent brewer's yeast β-glucans for potential applications in the food industry*. International Journal of Food Science and Technology 39(1), 21-29.

Tosh, S., Brummer, Y., Miller, S., Regand, A., Defelice, C., Duss, R., Wolever, T., Wood, P. (2010). *Processing Affects the Physicochemical Properties of β-Glucan in Oat Bran Cereal*. Journal of Agricultural and Food Chemistry 58, 7723-7730.

Ullrich, S. E., 2011, "*Barley: Production, Improvement, and Uses*". 1st Edition. Wiley-Blackwell.

Watkins, E., & Schweitzer, J.P. (2018). *Moving towards a circular economy for plastics in the EU by 2030*. In Think 2030: Institute for European Environmental Policy (IEEP) Brussels. (PDF reference downloaded on June 13th 2020).

Yoo, S. R., Krochta, J. M. (2011). *Whey protein–polysaccharide blended edible film formation and barrier, tensile, thermal and transparency properties*. Journal of the Science of Food and Agriculture 91(14), 2628-2636.

Zechner-Krpan, V., Vlatka, P., Panjkota-Krbavčić, I., Grba, S., & Berković, K. (2009). *Potential application of yeast β-glucans in food industry*. Agriculturae Conspectus Scientificus 74(4), 277-282.

Zechner-Krpan, V., Vlatka, P., Petra, G., Vanja, G., Filipovic-Grcic, J., Srečec, S. (2010). *Application of Different Drying Methods on β-Glucan Isolated from Spent Brewer's Yeast Using Alkaline Procedure*. Agriculturae Conspectus Scientificus 75(1), 45-50.

Zhang, Y., & Han, J. (2010). *Crystallization of high-amylose starch by the addition of plasticizers at low and intermediate concentrations*. Journal of Food Science 75(1), 8-16.

Zhu, F., Du, B., & Xu, B. (2016). *A critical review on production and industrial applications of beta-glucans*. Food Hydrocolloids 52, 275-288.

Zimkus A. & Chaustova, L. (2003). "*The permeability of Saccharomyces cerevisiae yeast strains with different cell wall architecture to lipophilic cation tetraphenylphosphonium and their transformation capability*". Biologija 3, 42-44.

Supplementary material

A- Differential scanning calorimetry

DSC, also known as quantitative DTA (differential thermal analysis) is a technique characterized by measuring the temperature interval between the sample and the reference, related with other variable (temperature or time), under controlled temperature settings. This temperature interval will be proportional to the thermal flow variation (amount of energetic input per time unit). The apparatus of a DSC system is described in Figure A 1 (Hatakeyama & Quinn, 1999).

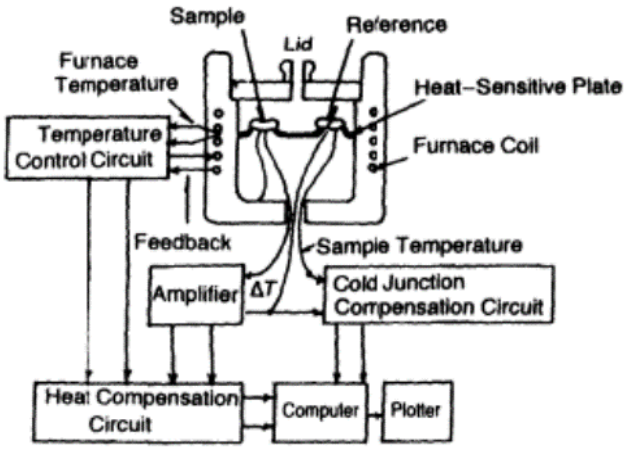

Figure A 1 Schematic representation of a DSC system.

The arrangement of the sample supporting set is different from what is found in a classic DTA. The thermosets are connected into the base of the sample and reference supports. Another pair of thermosets measures the temperature of the furnace and of the heat-sensitive plate. The basic principle of this technique is during physical transformation, when a change of phase occurs in which the sample will absorb or release heat, altering the thermal flux that goes through the heat-sensitive plate (Hatakeyama & Quinn, 1999). The thermal flux variation causes the temperature difference that represents an interval that will be measured between the plate and the furnace. If it is a positive interval, then the process will be exothermic; otherwise the interval is negative and therefore, the process is endothermic. The physical changes associated with the process are verified in Figure A 2 (Kaliappan, 2007).

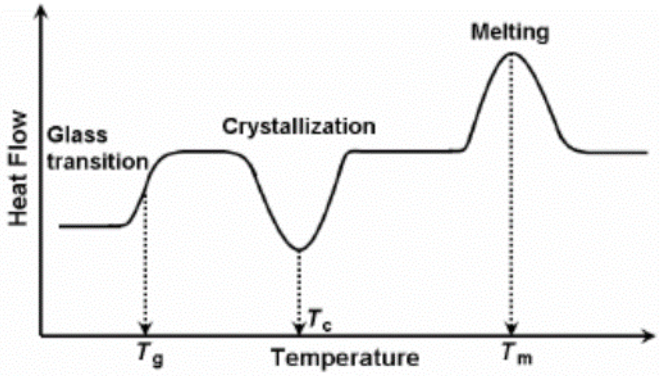

Figure A 2 DSC thermogram: measurement of thermal flux related to the temperature of a semi-crystalline polymer.

As shown in the figure, the curve depicts the endothermal glass transition region, the exothermal crystallization process, and the endothermal melting process. When a sample goes from the solid to the liquid state, it will require a larger thermal flux to increase its temperature comparatively to the temperature conditions that the reference is subjected to. This is due to the heat absorption by the sample during the phase transition. The opposite effect occurs in an exothermal process (such as crystallization), where lower thermal heat is required to increase the sample's temperature. By observing the thermal flux difference between the sample and the reference, it will be possible to measure the amount of energy released or absorbed with the aid of a calorimeter. Graphically, these "leaps" of energy are well defined and easily identified since there will also be notorious differences in the thermal capacity of the polymer either in glass or liquid state (Kaliappan, 2007).

The thermal analysis of semi-crystalline and amorphous polymers reveals different singularities. When the polymer is semi-crystalline, the melting temperature is a parallel temperature to the glass transition temperature since the latter is only verified in amorphous polymers. Another difference is that only the semi-crystalline polymer shows a well-distinct melting point. Both cases are depicted in Figure A 3 and Figure A 4, respectively (Silva, 2017).

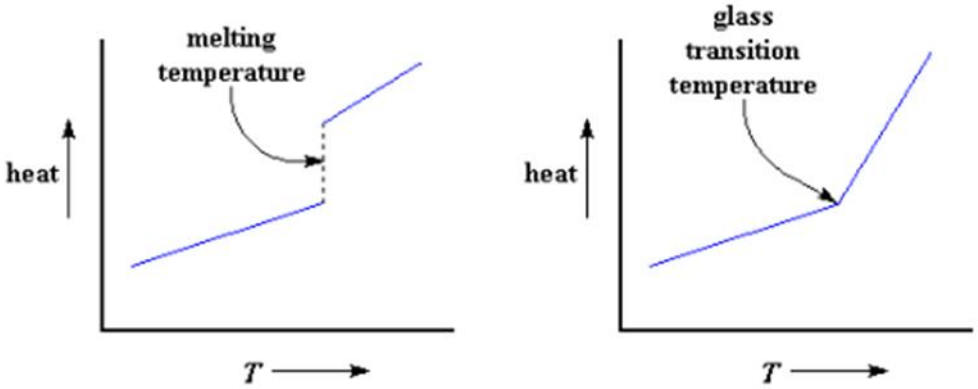

Figure A 3 Thermal flux varying with temperature, for a semi-crystalline polymer (left) versus an amorphous polymer (right).

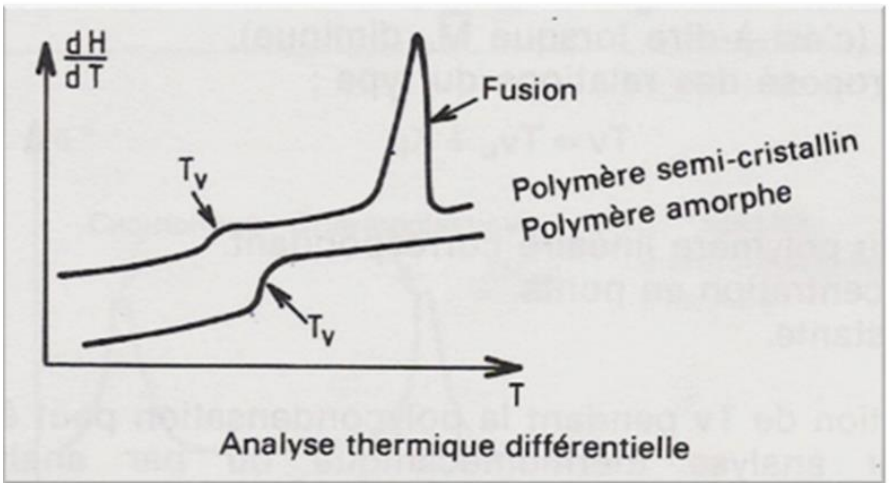

Figure A 4 Differential thermal analysis of a semi-crystalline and an amorphous polymer.

The peaks represented in Figure A 4 may be mathematically solved. The area above the peak's baseline may be answered by an integral equation, that provides the total enthalpic variation for the process(es):

$$\int \left(\frac{dH}{dt}\right)_{sample} dt = \Delta H_{sample} \qquad \text{(Eq. A.1)}$$

where $\frac{dH}{dt}$ is the enthalpic variation in function of time, and ΔH is the peak's enthalpic variation (Colby College, 2020).

The thermal capacity and its variations may be determined by observing the changes in the thermogram's baseline position. The thermal capacity is defined as:

$$c_p = \left(\frac{dq}{dT}\right)_P = \left(\frac{dH}{dT}\right)_P \qquad \text{(Eq. A.2)}$$

in which $\left(\frac{dq}{dT}\right)_P$ is the heat variation along the applied temperature, at a constant pressure (Colby College, 2020).

The thermal gradient, frequently mentioned as scan rate is given by:

$$scan\ rate = \frac{dT}{dt} \qquad \text{(Eq. A.3)}$$

Using function composition, comes the following equation:

$$c_p = \left(\frac{dH}{dT}\right)_P = \frac{dH}{dt}\ \frac{dt}{dT} \qquad \text{(Eq. A.4)}$$

where the last derivative is the inverse of the scan rate definition (Colby College, 2020). For differential measurements, the difference between the thermal capacity of the sample and the reference is determined:

$$\Delta C_p = \Delta \left(\frac{dH}{dT}\right)_P = \Delta \frac{dH}{dt}\ \frac{dt}{dT} \qquad \text{(Eq. A.5)}$$

where $\Delta \frac{dH}{dt}$ corresponds to the thermogram's baseline variation. The thermal flux units are normally expressed as kcal s^{-1} and the thermal gradient is expressed as °C min^{-1}. To be consistent with units, it will be required to change minutes to seconds or vice-versa (Colby College, 2020):

$$\Delta \mathrm{C_p} = \left(\frac{\mathrm{cal}}{\mathrm{s}}\right)\left(\frac{\mathrm{min}}{\mathrm{°C}}\right)\left(\frac{60\ \mathrm{s}}{\mathrm{min}}\right) \qquad \text{(Eq. A.6)}$$

Supplementary material

B- Thermogravimetric analysis (TGA)

TGA is used to investigate the thermal stability (resistance to degradation, at a determined temperature), oxidative stability (oxygen absorption rate) and compositional properties (such as additives, solvents, plasticizers, etc.) of polymeric materials. The mass gain occurs due to adsorption or oxidation, while the loss of mass is related to processes of decomposition, desorption, dehydration, solvation, and volatilization. This methodology is especially important in applications that use these polymeric materials such as injection molding for bottles, encapsulated materials for electrical and electronic components, dyes, adhesives, and some other industries such as food and pharmaceutical industries. The apparatus used in this technique is summarily depicted in Figure B 1 (Ng et al., 2002).

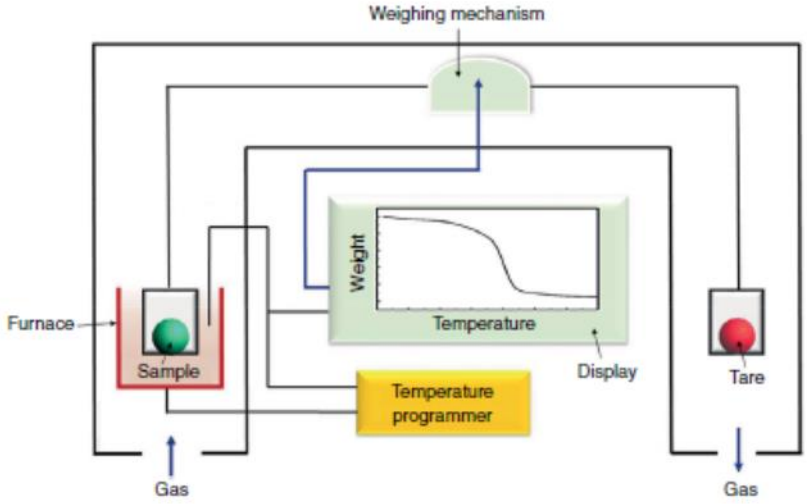

Figure B 1 Schematic diagram of a TGA instrument.

The theory behind this technique refers that TGA studies the samples' mass changes while its heated or cooled at a controlled temperature, T(t). The program that monitors the temperature may be isothermal (T(t)is therefore constant) or non-isothermal. The heating rate (β) may be expressed as:

$$\beta = \frac{dT}{dt} \qquad \text{(Eq. B.1)}$$

where dT is the temperature variation and dt is the time variation (Ng *et al*., 2002).

The mechanism and kinetics of the process related to the sample's mass variations may influence the shape and position of the thermogravimetric curves. Three of the variables that can influence the kinetic of the process are the temperature (T), the reaction's extension of conversion (α) and pressure (P). These variables can be implicitly shown as:

$$\frac{d\alpha}{dt} = k(T) * f(\alpha) * h(P) \qquad \text{(Eq. B.2)}$$

Despite the possibility that pressure has a considerable effect in the kinetic process, h(P) is commonly considered as insignificant in kinetic simulations (h(P) = constant, i.e., the environment is the equilibrium itself). This happens when all the reactive gas that reacts with the sample is removed (usually by purging with high flows of inert gas) (Ng *et al.*, 2002).

If the pressure has no effect on kinetics whatsoever, the function will have two variables, T and α:

$$\frac{d\alpha}{dt} = k(T) * f(\alpha) \qquad \text{(Eq. B.3)}$$

where k(T) represents the kinetic constant that is temperature dependent and f(α) is the conversion that will be dependent on the reaction model. The extent of conversion of the reaction is determined through a mass fraction difference:

$$\alpha = \frac{mi-m}{mi-mf} \qquad \text{(Eq. B.4)}$$

where m_i and m_f are the initial and final mass of the sample, respectively. The value of α may vary between 0 and 1, being caused by the general transformation from the beginning (materials) until the end (products) (Ng *et al.*, 2002).

The variation of temperature with the kinetic coefficient normally obeys the Arrhenius equation:

$$k(T) = A \exp\left(-\frac{E}{RT}\right) \qquad \text{(Eq. B.5)}$$

where A and E are kinetic parameters that correspond to the reaction's pre-exponential factor and activation energy, respectively. The gas universal constant is known as R, and T is the temperature (in Kelvin) programmed in the thermogravimetric analysis (Ng *et al.*, 2002).

An isothermal thermogravimetric curve may be presented by the following equation:

$$g(\alpha) = \int_0^x \frac{d\alpha}{f(\alpha)} = A \exp\left(-\frac{E}{RT}\right) t \qquad \text{(Eq. B.6)}$$

where g(α) is the integrated form in the reaction model. The equation may be obtained by substituting Equation 11 into Equation 9, followed by integration as it is indicated. In isothermal conditions, it would occur only variation of the value of α throughout the experiment. The reaction models may be categorized in three different profiles: (1) acceleration, (2) deacceleration and (3) sigmoidal (Ng *et al.*, 2002). The three models are shown in Figure B 2:

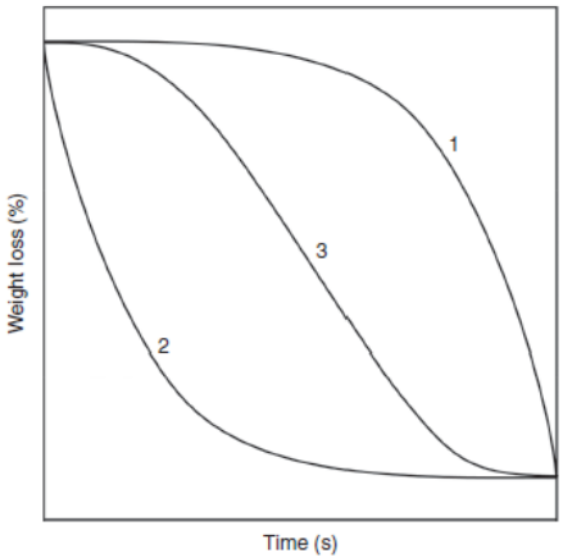

Figure B 2 Reactive models of acceleration (1), deacceleration (2) and sigmoidal (3) represented by the mass loss throughout time.

The acceleration models may be identified when the mass loss rate increases continuously during process, and the equation that represents it is the following:

$$g(\alpha) = \alpha^{n-1} \qquad \text{(Eq. B.7)}$$

where n is a constant value.

The deacceleration model is represented when the mass loss rate decreases throughout the process and the equation that represents it is the following:

$$g(\alpha) = \frac{1-(1-\alpha)^{(1-n)}}{1-n} \qquad \text{(Eq. B.8)}$$

where n is a reaction order ≠ 1 (for n = 1, g (α) = - ln (1- α)).

The Avrami-Erofeev model is applied in sigmoidal models since this model describes processes in which the sample's mass loss rate reaches its maximum point in intermediate values of the conversion process (Ng *et al.*, 2002). This model is represented by the following equation:

$$g(\alpha) = [-\ln(1-\alpha)]^{\frac{1}{n}} \qquad \text{(Eq. B.9)}$$

A non-isothermal curve model can also be described by substitution of Equation B.5 into Equation B.3, followed by integration, originating a final equation that describes the model as the equation below:

$$g(\alpha) = \frac{A}{\beta}\int_0^T \exp\left(-\frac{E}{RT}\right) dT \qquad \text{(Eq. B.10)}$$

Note that the graphical form of this model does not have any relation with the reaction model (3). For non-isothermal conditions, the heating rate keeps being constant due to the simultaneous variation of T e α. This condition contradicts the sigmoidal reaction conditions, where it shows an acceleratory phase followed by an deacceleratory phase (Ng *et al.*, 2002).

Supplementary material

C- Water retention kinetics and sorption isotherms

In general, hydrophilic films show water sorption isotherms with a small increment in the water content for low activity values (a_w) and a significative increment when $a_w > 0.6$. This sorption isotherm behavior suggests that the film hydration is presented in a multilayer arrangement, with a smaller amount of water strongly bonded to the polymer matrix that forms the monolayer and the majority of the water content is distributed in multilayers, that are indirectly bonded to the matrix. Thus, the water content is subjected to be transported by diffusion mechanisms (Delgado *et al.*, 2018).

The study of water transport properties is essential for a better understanding and possibly optimizing the protective functions of the film's membranes. If the control and prediction of the film's water content is incorrect, this can act as a plasticizer by incorporating water between the polymeric chains, increasing the spacing between them and consequently decreasing the glass transition temperature and affecting the chain's flexibility. The water transport does not occur between pores, but it can be understood through a simplified model that proposes that the process occurs in four stages: (1) water vapor absorption onto the polymeric matrix surface; (2)water vapor solution in the polymeric matrix; (3) water vapor diffusion through the matrix; (4) water vapor desorption through the opposite surface of the film (Delgado *et al.*, 2018).

The water sorption isotherms aim to study the water retention capability in equilibrium with the variable of interest which can be the relative humidity (r.h.) or activity (a_w = % r.h. /100) of the surrounding environment. The intrinsic water content of the film is normally evaluated through an activity function (a_w), by mass difference of the hydrated film and the totally dried film. The Guggenheim-Anderson-De Boer (GAB) model is frequently used in this field of application, with the goal of calculate the several variables that are shown in the isotherms:

$$h(a_w) = \frac{N*c*k*a_w}{[(1+(c-1)k*a_w)(1-k*a_w)]} \qquad \text{(Eq. C.1)}$$

where $h(a_w)$ is the water content based on the activity, N is the monolayer water content (g of water per g of dry basis mass), related to the primary location where water molecules bond, c is a parameter related with the sorption heat in the monolayer (also interpreted as the capability

of water bonding onto the monolayer) and finally k is a variable that is related to the multilayer sorption heat (or capability of water bonding onto the multilayer) (Delgado *et al*., 2016).

As to the water sorption kinetics, conventional chemical reaction's kinetic models are normally used. One of the most used models is the first order reaction model, having into account two processes with distinct water retention ratios:

$$h(t) = h_0 + A_1\left[1 - \exp\left(-\frac{t}{\tau_1}\right)\right] + A_2\left[1 - \exp\left(-\frac{t}{\tau_2}\right)\right] \qquad \text{(Eq. C.2)}$$

where h(t) is the water content as a function of time, h_0 is the initial water content, A_1 and A_2 are kinetic constants and τ_1 and τ_2 are time constants related to the water retention of process 1 and 2, respectively (Delgado *et al*., 2016).

Another frequent used model is the one that determines the water content as a function of time, adding a Fick's differential mass transport law in a Fourier series (infinite plate) where water diffusion occurs in an unidimensional form:

$$h(t) = h_\infty\left\{1 - \sum_{n=0}^{\infty}\frac{8}{(2n+1)^2\pi^2}\exp\left[-D_w^{eff}(2n+1)^2\frac{\pi^2 t}{4L^2}\right]\right\} \qquad \text{(Eq. C.3)}$$

where h_∞ is the equilibrium water content, L is the film's thickness, and D_w^{eff} is the apparent diffusivity coefficient (m^2*s^{-1}) (Delgado *et al.*, 2018).

The STL (short time lapse) model is another alternative, used mainly for water sorption studies at the beginning of the experimental period. It is described by the following equation:

$$h(t) = 2h_\infty\left(\frac{D_w^i t}{\pi L^2}\right)^{1/2} \qquad \text{(Eq. B.4)}$$

This equation is valid for sorption data when $h(t)/h_\infty < 2/3$. It is considered as an initial period of study up to 12 hours (Delgado *et al*., 2018).

There are also equations that describe the type of transport phenomena that happens in the film. One of them is the Korsmeyer-Peppas model, given by the following equation:

$$h(t) = h_\infty k t^n \qquad \text{(Eq. B.5)}$$

where k is a constant that depends on the matrix's characteristics, and n is the diffusional exponent. The equation becomes valid when $h(t)/h_\infty < 2/3$. This equation is based on Equation B.4 because when n is equal to 0.5, both equations become essentially the same and the

transport is purely ideal. Thus, n is the essential indicator of how the process is deviated from what is considered ideal transport and it will determine the type of diffusion in the film (Delgado *et al*., 2018):

- $0 < n \leq 0.5$: quasi-fickian or fickian diffusion
- $n = 0.5$: ideal diffusion
- $0.5 < n \leq 1$: non-fickian or anomalous diffusion (where water diffusion is much faster compared to the molecular relaxation process of polymeric chains since the latter is the main regulatory sorption process.

Finally, to determine water vapor permeability of the film, it is required to determine the film's water solubility. According to Henry's law, water solubility (S_w) at a film's 90% relative humidity is given by the following equation:

$$S_w = \beta \rho_{d.f.} = \frac{h_\infty}{p_s} \rho_{d.f.} \qquad \text{(Eq. B.6)}$$

When it is considered that there are no pores, cracks or holes in the film, permeability (P) can be expressed by multiplying the diffusion coefficient (D) and the solubility coefficient (S). Therefore, water vapor permeability is defined by:

$$P_w = D_w S_w \qquad \text{(Eq. B.7)}$$

Where P_w is expressed in g s^{-1} m^{-1} Pa^{-1}, S_w and D_w can be obtained from equations B.6 and B.4, respectively. In an ideal case, permeability is an intrinsic attribute of the film when the diffusivity and solubility coefficients are not influenced by the content of the permeated component. In a practical view, the permeate interacts with the film's matrix, despite the solubility and the diffusivity being influenced by different partial pressures between the film's surfaces (Delgado *et al*., 2018).

Supplementary material

D- Oxygen permeability: experimental procedure

These conditions were tested by Muramatsu *et al.* (2003). The co-polymer tested was ethylene-vinyl alcohol, which is different from the polysaccharide and protein-based film that is being investigated. However, in order to understand the methodology and result analysis of oxygen permeability dependent on temperature and relative humidity, this research will be considered valuable since results can be analogous to those of a polysaccharide or protein-based polymer.

The equipment used involved an oxygen permeation analyzer (OPA) to measure oxygen permeability. A positron annihilation lifetime spectroscopy technique (PALS) was also applied to check free volume hole size in the film. Oxygen permeability dependent on temperature was measured between 20 to 80 ºC with the OPA apparatus. Free volume was measured from -150 ºC to 150 ºC. For the relative humidity dependence experiments, samples are kept under constant humidity for 1 month at 20 ºC (ambient temperature) in order to reach a water vapor equilibrium with the surrounding environment, and only after they will be measured under different percentages of relative humidity. The final results are shown in Figure D 1 and Figure D 2 below (Muramatsu *et al*., 2003):

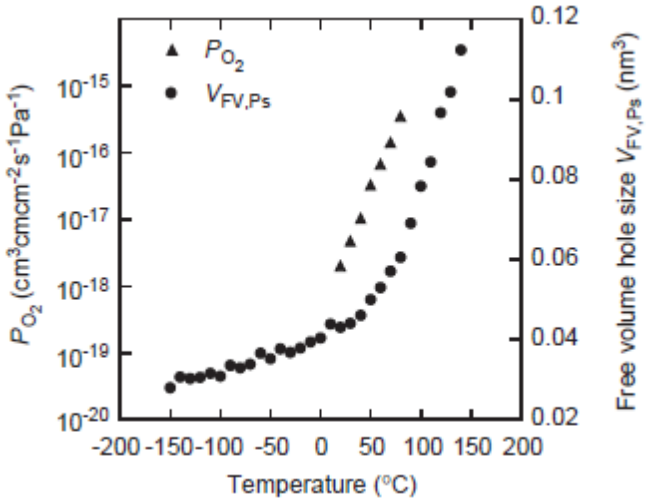

Figure D 1 Temperature dependence of oxygen permeability coefficient and free volume hole size.

It can be seen that oxygen permeability increases exponentially as a function of temperature, without significative changes at 56 ºC (glass transition temperature of the polymer). Above 56 ºC, the high crystallinity degree is supposed to decrease oxygen permeability. However, the influence of the degree of crystallinity is usually smaller compared to the influence of temperature since this one follows an Arrhenius type model that exponentially increases the weight of the temperature variable.

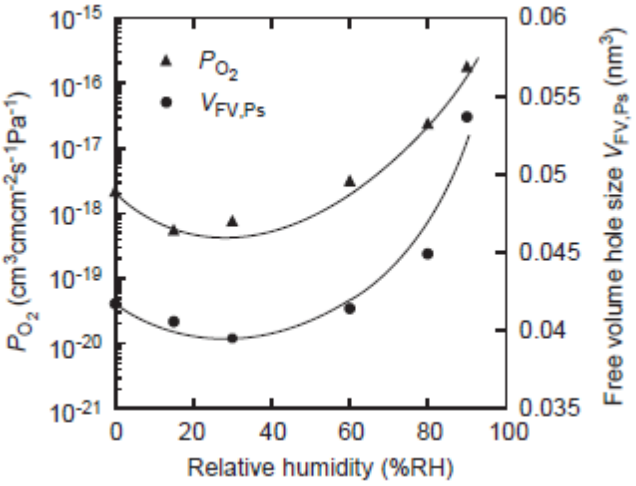

Figure D 2 Humidity dependence of oxygen permeability coefficient and free volume hole size.

In this scenario, oxygen permeability decreases when relative humidity increases from 0 to 25%. After 25% oxygen permeability increases, and at 90% of relative humidity is around one hundred times larger than 0%. In addition, the behavior of oxygen permeability is quite similar to the free volume hole size. It is suggested that from 0 to 25%, water molecules fill the free volume holes, not allowing oxygen to permeate and at the high humidity region, both free volume and oxygen permeability increase due to the plasticizing effect of water molecules.